

Life cycle climate change impacts of producing battery metals from land ores versus deep-sea polymetallic nodules



Daina Paulikas ^{a, *}, Steven Katona ^b, Erika Ilves ^c, Saleem H. Ali ^{a, d}

^a Minerals, Materials and Society Program, University of Delaware, Newark, DE, 19716, United States

^b College of the Atlantic (emeritus), 105 Eden St, Bar Harbor, ME, 04609, United States

^c Deep Green Metals Inc, 10th Floor, 595 Howe Street, Vancouver, British Columbia, V6C 2T5, Canada

^d Sustainable Minerals Institute, Level 4, Sir James Foots Building (No. 47A), The University of Queensland, St Lucia, QLD, 4072, Australia

ARTICLE INFO

Article history:

Received 6 April 2020

Received in revised form

24 July 2020

Accepted 15 August 2020

Available online 28 August 2020

Handling editor M.T. Moreira

Keywords:

Life cycle assessment

Mining

Metal

Polymetallic nodules

Climate change

Carbon sequestration

1. Introduction

A new, abundant, and high-grade polymetallic source of metals for the clean-energy transition could come on-stream in the next few years. The International Seabed Authority (ISA), established pursuant to the United Nations Convention on the Law of the Sea (UNCLOS), has awarded over a dozen exploration contracts for the collection of deep-sea polymetallic nodules from the Clarion Cliperton Zone (CCZ) and is now poised to adopt regulations for commercial exploitation (ISA, 2019). The potential commencement of deep-sea mining (DSM) of nodules has been met with opposition from Greenpeace and other NGOs concerned about biodiversity loss and ecosystem and carbon-cycle disruptions in the ocean (Greenpeace, 2019). To date, this DSM debate has narrowly focused on ocean impacts from the nodule-collection phase, whereas direct and indirect planetary-scale impacts and full life cycle impacts of

production including onshore processing have been largely absent from consideration. Nor have the impacts of nodule collection been compared to current practice: using conventional metal-bearing ores on land to supply primary metal demand. In the short-to-medium term, the bulk of new metal demand resulting from a metal-intensive clean-energy transition, population growth, and development will not be compressible, nor can this demand be supplied by recycling efforts alone (Hund et al., 2020). Until sufficient metal stocks are built up in the global system, a primary metal source is required to meet the new demand. Which primary metal source would create the least damage to the planet and its people: land ores or deep-sea polymetallic nodules? A comparative life cycle assessment (LCA) grounded in a planetary perspective is needed to answer this question and to help inform discourse on the consequences of entering the deep sea.

This paper begins to address these gaps. It follows established LCA methods to extend the current analysis of metal production to the CCZ nodule resource. LCA is a widely used, ISO-based scientific methodology for assessing comparative environmental impacts. It considers the direct and indirect contributions from materials, energy, transport, and other process inputs to compute an aggregate impact for a number of standardized indicators. Taking the consumption unit as a given so that any behavioral shifts, crowding-out effects, or policy externalities are isolated from study (Yang, 2017), a “cradle-to-gate” (from resource to refined metal) LCA enables a direct, apples-to-apples impact comparison of producing the same material from two different sources. Given the urgency of the climate crisis, this paper quantifies impacts on climate change: it shares the results of the first cradle-to-gate LCA of metal production from polymetallic nodules with a focus on global warming potential (GWP) and carbon-sequestration cycle impacts, and compares them to land-ore mining.

Several types of metal-bearing deposits have been explored in the deep sea—seafloor massive sulfides, cobalt crusts, seabed sediments, and polymetallic nodules—each with a unique environmental and economic footprint. Polymetallic nodules are of particular interest because they (1) occur in or on soft seabed sediment, unattached to the ocean floor, and can be collected

* Corresponding author.

E-mail addresses: daina.paulikas@gmail.com (D. Paulikas), steven.katona1@gmail.com (S. Katona), erika@deep.green (E. Ilves), saleem@udel.edu (S.H. Ali).

without destructive rock cutting (Secretariat of the Pacific Community, 2013); (2) contain high-to-medium grades of four metals in a single ore and do not contain toxic levels of heavy elements (Haynes et al., 1985); (3) have metal contents serendipitously aligned with the metal needs of electric vehicle (EV) battery and assembly manufacturers—nickel, cobalt, manganese, and copper (AMY, 2018); and (4) are present in vast enough quantities within the surveyed CCZ to become a major source of battery metals for the coming decades. The CCZ represents 1.5% of the world's abyssal plains and hosts on its surface 34 billion wet metric tons of nodules containing 6 billion tons of manganese, 270 million tons of nickel, 234 million tons of copper, and 46 million tons of cobalt (Morgan, 2000). Allowing for protected areas and process inefficiencies, if half of these nodules were collected, the total commercial value of contained metals would be around 5 trillion US dollars (USD), based on average long-term projected commodity prices (AMC Consultants, 2019a).

The issue of DSM is particularly critical given present economic and environmental circumstances. The global green transition is pressuring supply chains of three of the nodule metals; meanwhile, the climate crisis dictates carbon consciousness in the very construction of this transition. Nickel sulfate and cobalt sulfate markets for energy storage are expected to grow more than fifteenfold from 2018 to 2035 (CRU International, 2019), largely driven by the need to build EV batteries. Nickel-manganese-cobalt (NMC) and other nickel-heavy battery chemistries are projected to dominate the EV supply chain in the coming decades (Bloomberg New Energy Finance, 2020). A single Tesla Model 3's 75 kWh NMC 811 lithium-ion battery cathode requires 56 kg of nickel in nickel sulfate (NiSO_4), 7 kg of cobalt in cobalt sulfate (CoSO_4), and 6.6 kg of manganese in manganese sulfate (MnSO_4), along with 85 kg of copper cathode for the harness and connectors (AMY, 2018)—or 155 kg of the four base metals found in CCZ nodules. Morgan Stanley projects the global EV passenger fleet to reach 1 billion units by 2047 (Morgan Stanley, 2017); 1 billion such EVs would require 155 metric megatons (Mt) of these metals. Even if NMC's dominance is disrupted, other key, green-transition activities—such as building the global renewable energy infrastructure—will still require vast amounts of the nodule metals (Hund et al., 2020).

This enormous new metal demand must come from primary sources (land ores or ocean minerals) and/or secondary sources (recycling or landfills). Studies strongly suggest that secondary sources will not suffice. With about 6 million EVs on the road globally, not enough readily usable stocks of recycled metals exist from which to build a billion EVs. The EV is a relatively new, exponentially growing product with a life span of 10+ years. Even a best-case assumption of 100% EV battery recycling cannot come close to filling the demand gap (Hund et al., 2020). Meanwhile, metal stocks contained in landfills are difficult to estimate and access economically. Hence, if the green transition is to proceed, a large new injection of primary metals extracted from the planet seems unavoidable. Yet, nickel and cobalt mined from land ores face great challenges in meeting this new demand, with too few projects in the development pipelines.

Meanwhile, the remaining carbon budget of 235 metric gigatons for a 66% chance of keeping global temperatures within 1.5 °C of pre-industrial levels (Nauels et al., 2019), or under seven years' worth of current emission rates (IPCC, 2018), means an urgency to minimize every gigaton of emissions of carbon dioxide and other heat-trapping gases. The metals produced for the green transition produce substantial life cycle emissions. The battery represents over two-thirds of the life cycle GWP of a manufactured EV, and about half of this is attributable to raw materials like battery metals (Hausfather, 2019). The climate change benefits of transitioning to

greener cars will be partially undermined by producing the very metals needed for it. Within this context, studies shedding light on the climate change impacts of metal production, like the present one, are urgently needed.

Further, the production of nickel sulfate has raised concerns about its high levels of toxicity, high GWP, habitat destruction, and biodiversity loss. Historically, nickel for battery-grade sulfate was primarily sourced from sulfidic deposits, but as these resources dwindled, production shifted to laterite deposits that are found in wet, hot, tropical areas with high species richness, thereby presenting a threat to biodiversity (Tardy, 1997). Today's largest producer of nickel, laterite-rich Indonesia, contains the world's third-largest rainforest area and globally ranks third in biodiversity (Rainforest Action Network, 2020). Known factors (Table 1) will drive the environmental and social impacts associated with metal production, whether from land or ocean sources; some factors are innate while others are controllable. Side-by-side land-ore and nodule processing phases (Table 2) illustrate the differences in impact drivers between the two sources.

Two topics are quantified and assessed in this paper: direct and indirect emissions measured as GWP, and disruptions to carbon-sequestration cycles. A robust body of academic and corporate LCA research exists on the GWP impacts of land-based metal production, including published literature on specific production pathways or pathway groups, and standard databases like Ecoinvent—a catalog of process, flow, and emissions data across sectors, including metals, transport, energy supply, and agriculture. Recently, Nuss and Eckelman (2014) developed LCAs for the production of 63 different metals, augmenting Ecoinvent v2 with updated byproduct allocations and production paths. Results are not static as key drivers may change over time; land-ore grade, carbon intensity of used energy, processing efficiency, electricity-grid carbonization, and geological composition can affect the material and energy inputs to production and the final result (Norgate et al., 2007; van der Voet et al., 2018). In response to this dynamics problem, researchers introduced life cycle sustainability assessments (LCSAs), adding a time dimension and including up to three sustainability pillars—environmental, economic, and social (Guinee 2016)—thereby increasing policy relevance. Recent studies including van der Voet et al. (2018), Kuipers et al. (2018), and Verboon (2016) used LCSAs to show that ore-grade declines may increase the GWP of metals like nickel and copper by 12–32% by 2050, while an aggressive global electricity-grid decarbonization could counter this trend and decrease GWP values by 4–33%. There is little published life cycle analysis on DSM to date, making it difficult to compare the two metal sources or validate climate change concerns raised by DSM-opposing voices. Heinrich et al. (2020) computed GWP for several scenarios of offshore nodule collection and ship transport, but the study stops short of full cradle-to-gate assessment by excluding the GWP-dominating onshore processing steps.

For analysis of the carbon-sequestration cycle impacts, both the release of already-sequestered carbon and reductions of future carbon-sequestration services were considered. On a planetary scale, terrestrial soils are the world's second-largest carbon sink (~2300 metric Gt), or 15 times larger than surface sediments of the abyssal seabed (~150 metric Gt), and second only to the intermediate and deep ocean (~37,100 metric Gt) (World Ocean Review, 2010). On land, carbon from dead roots and trees, fallen leaves, and other vegetation enters soil over time, and if left undisturbed the soil sequesters this carbon over long periods (EEA, 2015). In the ocean, sequestered carbon takes numerous forms: detritus that has sunk through the water column accumulates on the seafloor; dissolved organic or inorganic carbon is contained in sediment pore water; carbon is stored in the bodies of bacteria that decompose

Table 1
Drivers of climate change and other environmental impacts of metal production.

Factor	Key questions
Biodiversity richness	How many individuals and distinct species reside in the areas targeted for resource extraction or processing? How resilient are they to disruption? Are many endemic?
Ecosystem-services integration	How important are the disrupted areas for ecosystem services (provisioning, regulating, supporting, and cultural) for humans?
Mineralogy	What is the physical and chemical makeup of the ore? Are beneficiation or coal-intensive reduction needed? Will reactions be endothermic, requiring more energy? Are large quantities of toxic elements present?
Processing plant location	Is the plant close to its end market? Can industrial byproducts be recycled and used by neighboring facilities? Can the plant be located next to running hydropower? Does the local electricity grid use renewables?
Transport requirements	Are trucks used? Are materials moved over extensive distances?
Flow-sheet design	Are environmentally optimized material, processing, and energy choices prioritized, and at what economic cost?
Waste production and management	How much solid waste is produced? How much is toxic? How much tailings and waste rock must be managed?
Operational excellence	How are tailings and waste streams managed? Is soil buried to reduce carbon release?
Mine closure and site remediation	How effective are remediation techniques? What regulations are in place? How often are sites properly closed?

detritus or that assimilate dissolved inorganic carbon, including carbon dioxide; accumulations of methane clathrate originate from anaerobic decomposition and are found all over the world in deep sediments along continental shelves overlain by highly productive surface waters, as well as in shallow waters of the Arctic and in sediments underlying Arctic permafrost; and reservoirs of carbon dioxide clathrate form from volcanic outgassing near active hydrothermal vents. Disruptions from mining land ores or collecting nodules, and from processing and refining the materials onshore, may cause atmospheric release of carbon that was previously sequestered, as well as reduce future sequestration activity as long as ecosystem conditions remain unrestored. Carbon sequestration has been raised as a topic of potential concern with nodule collection, though, as with GWP, little has been published on the topic for DSM.

This paper is anchored by a demand scenario that creates a clear side-by-side comparison of land ores versus deep-sea nodules for producing battery metals for 1 billion EV batteries and connectors by 2047. For land ores, an LCA baseline was developed based on published literature and incorporating ore-grade declines, energy-efficiency improvements, and electricity-grid decarbonization dynamics. For nodules, an original LCA model was created based on in-depth, independently compiled engineering studies and preliminary economic assessments for a planned nodule-collection operation in the CCZ. GWP and carbon-sequestration cycle impacts were quantified for both sources within the context of 1 billion EVs.

To the authors' knowledge, this paper represents the first published attempt to (1) create a cradle-to-gate LCA of metal production from deep-sea polymetallic nodules; (2) construct a representative LCA for the base metals necessary for an EV battery plus copper harness and connectors, including projected supply and demand dynamics; (3) quantify the carbon-sequestration cycle impacts of producing metals from deep-sea polymetallic nodules; and (4) compare the environmental impacts of producing metals from primary land ore sources versus from deep-sea polymetallic nodules.

2. Methods

2.1. GWP assessment methods

ISO 14040/44 guidelines are followed below to describe the formation of LCA baselines for both land-ore and polymetallic-nodule sources. As climate change is the focal point of this investigation, the life cycle impact assessment (LCIA) indicator "GWP 100a" was analyzed first—a typical first-studied indicator in a metal-production LCA.

2.1.1. LCA goal and scope

The objective of this LCA study is to assess the climate change impacts of producing four metals needed for 1 billion EVs over the period 2017 to 2047, in a comparative study of two metal source types—land ores and deep-sea polymetallic nodules. Intended audiences include industry participants, the ISA and other policy-makers, NGOs, environmental organizations, LCA practitioners, and academics. The study scope is cradle to gate, enabling side-by-side comparison of impacts from producing a kilogram (kg) of the same refined metal. Included in the system boundary are metal extraction, transport of intermediate ore product and some individual raw materials, hydrometallurgical or pyrometallurgical ore processing, and metal refining (e.g., purification, electrorefining, crystallization), along with mine and plant infrastructure and material and energy inputs. Further details are noted in Supplementary Data. The basic unit of measure is 1 kg of metal contained in final compound form: three base metals in battery-grade format needed for NMC 811 batteries—nickel sulfate, cobalt sulfate, and manganese sulfate—and copper cathode (high-purity commoditized copper) used in EV harnesses and connectors. For land ores, following van der Voet et al. (2018), Kuipers et al. (2018), and Verboon (2016), two supply scenarios are studied: a baseline scenario, in which business-as-usual policies are followed globally while declining ore grades worsen climate change impacts; and a green scenario, in which massive grid decarbonization of the background electricity mixes offers an optimistic case. For deep-sea polymetallic nodules, one static supply scenario is used throughout: a defined "planned project scenario" that exploits a zero-waste processing flow-sheet design and hydropower for onshore processing. Ore-grade dynamics are not modeled for nodules, as their grades are estimated to be relatively consistent across the CCZ (AMC Consultants, 2019a).

2.1.2. LCA methods

For land ores, a baseline of per kg GWP impacts of each of the four metals in final-study-compound form was developed by surveying published metal LCA research and databases; selecting production paths based on relevance to battery-grade metal production, data availability, and data recency; where necessary, modeling additional process steps to take metal compound end points to the correct, final-studied-compound forms (e.g., taking a pure metal to a sulfate); and weighting the paths based on trends in resources and production. Secondary production paths (recycling) were excluded from study; the nature of the question at hand requires inclusion of extraction, and LCA impacts of recycling would be the same regardless of initial primary source. Separately, a baseline of per kg GWP impacts of each metal in final-study-compound form produced from nodules was created by collecting

Table 2
Innate and controllable process differences—comparison between land ores and nodules.

Land ores	Deep-sea nodules
Mining stage: Exploration	
<ul style="list-style-type: none"> Prospecting is high risk, with no major discoveries of tier I mining assets made over the last decade. Prospecting involves remote sensing of geological structures and on-site drilling into hard rock to collect drill cores to test for composition. 	<ul style="list-style-type: none"> Prospecting is less risky, with several nodule deposits identified (e.g., the CCZ, the Peru Basin, the Central Indian Ocean Basin) and characterized as high grade and high abundance. Most of the ~20 ISA nodule exploration contract areas would be classified as tier I deposits. Prospecting involves observing the seafloor using sensors mounted on vessel hulls and/or autonomous underwater vehicles, and collection of nodule and biological samples.
Mining stage: Development	
<ul style="list-style-type: none"> If the mine site is in a remote location, new infrastructure is built and maintained (roads, bridges, power, water, miner accommodation). Underground mines require drilling of access shafts and tunnel networks. Open-pit mines require clearing forests or other vegetation and removing topsoil to access the ore body. To build a terraced access to the ore body, a much larger area needs to be excavated, with stripping ratios of 1–10 tons of waste rock for every ton of ore body not uncommon. If the site is populated, communities are resettled. Development of a mine can take more than five years. 	<ul style="list-style-type: none"> Development involves building an offshore production system (surface vessel, vertical lift system, seabed collection machines). Manufacture of each offshore production system can take up to two years. This does not include initial system design phases and pilot mining systems development, which may take three or four years. Full-scale system design can take an additional year, though subsequent systems would be iteratively designed on tighter timelines as learning and improvement take place, as with any large-scale system development.
Mining stage: Ore extraction or collection	
<ul style="list-style-type: none"> The most common method used to excavate a metal-bearing ore body is to drill holes into hard rock, fill them with chemical explosives, and blast. Resulting fragments of blasted rock are then fed into a crusher and, in the case of sulfide ores, can be chemically concentrated on-site. Mining disrupts tracts of land at the mining site and for connecting roads. Mining for base metals increasingly takes place in some of the most biodiverse places on the planet. Transport is primarily by truck to remote locations. Particulates and harmful dust are released into the atmosphere, with noted health risks to miners and surrounding communities. Substantial amounts of freshwater are drawn from lakes, streams, and groundwater sources. Contamination of groundwater can result in human and wildlife illness and death. Marine-water impact consists of runoff pollution, especially from near-coastal mines, possibly harming marine animals. Deep-sea tailings placement can also impose a major marine impact. Communities are impacted because mining sites may be near local inhabitants; direct physical harm or cultural disruption may occur. Communities can also benefit because mining can bring development and industry to remote areas. Waste streams are commonly produced in large quantities from mining and concentration, often putting communities, wildlife, and habitats at risk locally and regionally. 	<ul style="list-style-type: none"> Nodules sit unattached in the top 5 cm of sediment. They are picked up by seabed collection machines, which may direct jets of deep seawater along the surface of the seabed to lift and channel nodules into the machine along a curved nozzle head using the Coanda effect (the pressure-differential effect that lifts airplanes off the ground). Nodules are separated from entrained sediment inside the collection machine and channeled into a vertical lift system; most separated sediment is discharged at the back of the collector. Nodules are transported to the surface production vessel using a vertical-lift system inside an enclosed riser pipe. Deep seawater from nodule transport containing residual fines is reinjected at a depth below 1000 m. Nodule collection removes the hard substrate of nodules. Some wildlife requires these substrates for attachment (“nodule obligates”), and some rely on these hard substrates for critical life functions (e.g., egg laying). The populations of these species will be disrupted in collection areas. Collection machine movement and sediment discharge generate plumes (i.e., suspended seabed sediment). As plumes resettle on the seabed, they can smother, kill, and disrupt wildlife in the impacted area, depending on the blanketing thickness. Transport is primarily by ship. Air impact is limited to typical ship emissions during operation. There is little direct freshwater impact. Marine-water impact includes reinjection of slightly warmed, decompressed deep seawater with turbidity, possibly harming ocean wildlife, as well as typical ship emissions, which include discharges into the water. No local communities are impacted as nodule collection takes place far from human populations. Nodule collection can provide jobs and economic benefit, with potential to aid developing nations who act as sponsoring states for ISA contractors.
Mining stage: Closure and reclamation	
<ul style="list-style-type: none"> Mine closure is costly to implement. It is often postponed indefinitely or not completed. Unrestored land further pollutes habitats, causes human illness, and prevents future habitats from redeveloping. Improper disposal of mining waste causes human and animal illness and death from acid mine drainage, toxic dusts, and groundwater pollution. Environmental protection measures and enforcement vary depending on the strength of the national and local governments, particularly in developing countries. 	<ul style="list-style-type: none"> Nodule collection can be stopped at short notice. Restoring disturbed seabed to its pre-collection state on human timescales presents substantial scientific and logistical challenges. No disasters or human illness or death are caused by leaving nodule-collection sites unrestored. Setting aside 30–50% of the area into preservation zones and leaving 15% of nodule cover in collection zones will aid natural habitat restoration, but the process will likely take a very long time and is dependent on habitat connectivity, still under study. Environmental protection measures are developed in consultation with a broad range of stakeholders and enforced by the ISA.
Processing stage	
<ul style="list-style-type: none"> Processing plants are usually located within trucking distance from the mine site (especially for bulk ores that cannot be concentrated easily at the mine site), mostly in developing countries, and are powered by local electricity grids that often rely on coal. Ores often contain toxic levels of heavy elements that need to be removed and stored during processing. Large volumes of processed tailings and residues from this phase require specially 	<ul style="list-style-type: none"> Processing plants can be located anywhere in the world with access to a deep-water port. Site selection can be optimized for access to renewables like hydropower. Nodules do not contain toxic levels of heavy elements and can be processed with no tailings, residues, or solid waste. Physical footprint consists of land occupied by a processing plant, as well as road building and maintenance.

Table 2 (continued)

Land ores	Deep-sea nodules
<ul style="list-style-type: none"> engineered facilities (tailings dams) and ongoing monitoring and maintenance indefinitely into the future. Physical footprint consists of land occupied by a processing plant, tailings dams, and residue storage facilities, as well as road building and maintenance. Some processing is constrained to the mine site while some is more distant. Impacts result from pyrometallurgical and/or hydrometallurgical processing and depend on the ore. Significant pollution and waste are generated from standard techniques. 	<ul style="list-style-type: none"> Impacts result from pyrometallurgical or hydrometallurgical processing. Processing can be optimized for low waste and emissions due to nodules' unique mineralogy and plant-location flexibility.
Refining stage	
<ul style="list-style-type: none"> Additional plants may need to be built for refining, with associated extra costs for transport and land use, and powered by local electricity grids. Tailings and residues may be produced by this phase. Refinery locations attempt to be optimized for transport to market. 	<ul style="list-style-type: none"> Hydrometallurgical refining is co-located with processing. Additional plants may be built for refining into other final products, with associated extra costs, powered by local grids. Intermediates can be processed with no tailings or residues. Transport to market minimizes the use of trucks due to location near a port for international market access.

foreground life cycle inventory (LCI) data into a model. The industry-standard LCA modeling tool SimaPro v9.0 was employed to implement the model and calculate LCIA indicators (Pre Consultants, 2020).

For land ores only, once per kg GWP impacts were calculated statically, the two aforementioned dynamic supply scenarios were created following the methodologies employed in the three referenced land-ore LCSA studies, thus producing a 2017 to 2047 time series of per kg impacts. Separately, combining the NMC 811 battery chemistry with Morgan Stanley's 1 billion EV demand projections (Morgan Stanley, 2017) yielded a base-metal-demand time series for each metal from 2017 to 2047. Integrating these metal-specific demand time series with the metal-specific impact time series yielded total GWP results for 1 billion EVs using land ores. For nodules, static per kg GWP values were multiplied by total metal quantities needed for 1 billion EVs.

2.1.3. Background LCI data

To ensure comparability, the same background LCI database was selected for the nodules model as is employed by the majority of land-ore baseline literature: Ecoinvent v2.2 (see version summary in (Ecoinvent, 2020)). Note that Ecoinvent v3 contains more recent and robust data and includes material-transport impacts natively. However, as most of the land-ore-baseline studies utilized Ecoinvent v2.2 despite these studies' recency, the v2.2 database was selected for the nodules model by necessity. In exceptional cases of data unavailability, Ecoinvent v3 entries were occasionally used, as indicated in Supplementary Data.

2.1.4. LCA allocation

When creating an LCA model, anytime a single processing step results in two or more outputs, the step's impact must be allocated. Consistency in allocation method is critical for comparability as LCA results can differ drastically depending on the choice. A breakdown of a CCZ nodule's main products by both mass and economic value illustrates this difference (Fig. 1): manganese accounts for over 80% of output by mass but only 22% by economic value; nickel accounts for less than 4% of output by mass but a full 50% by economic value. These differences somewhat lessen under final allocation, as any separable subprocesses are first allocated directly or physically per ISO 14040/44 guidelines.

Arguments for mass-based allocation include commodity price volatility (multiyear moving averages are commonly used) and the intuition that physical proportions are relevant. Arguments for economic allocation include that economics are the impetus for the activity and that a product's price reflects its relative utility. LCA

allocation based on economic value is the method of choice in metal production LCA literature; this paper follows common practice by leading with economic allocation while also including mass-based sensitivity analyses (Guinee et al., 2002).

2.1.5. Land-ore model and foreground LCI data

The literature comparables and production paths used to construct the land-ore baseline are provided below and summarized in Table 3. Path weights were based on geographical and geological production trends, reserve ratios, literature review, and practitioner judgment. LCI data and references for the land-ore baseline along with production-path details are found in Supplementary Data.

2.1.5.1. Nickel sulfate. Given their comprehensiveness, recency, and production path relevance, van der Voet et al. (2018) and Verboon (2016) were used for the nickel sulfate baseline. These studies include a robust LCA and LCSA for Class 1 nickel (required quality for battery-grade nickel sulfate) and augment an Ecoinvent starting point with numerous literature sources and recent process data. Two representative battery-grade nickel routes from these papers were used: a pyrosulfidic route mined from underground, using flotation and drying, smelting in a flash furnace, and hydrogen-sulfide reduction (the Sherritt process) for refining, with a copper coproduct; and a hydrolateritic route mined from an open-pit surface mine, with no concentration or drying due to its higher ore grade, using high pressure acid leaching and solvent extraction/electrowinning for refining, with no coproducts.

As of 2010, around 86% of Class 1 nickel production came from pyrosulfidic production. Laterites are gaining overall nickel market

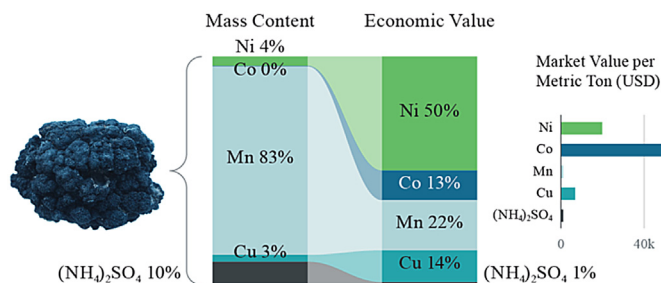


Fig. 1. Mass-based and economic output from CCZ polymetallic nodules. Average price projections from 2025 to 2055 estimated by CRU International are given per metal amount contained in final-product forms (CRU International, 2019). Nodule contents are based on analysis for NORI Area D (AMC Consultants, 2019a).

Table 3
Land-ore baseline model production paths included.

	Pathway description	Ore type	Mine type	Process type	Model adjustments	Geographies	Price data for allocation	Transportation included	Infrastructure included
Nickel sulfate	Class 1 Ni, produced pyrosulfidically, converted into sulfate	Sulfates with Cu coproduct	Underground	Pyro	Sulfate crystallization add-on	Variety of global locations aggregated by studies cited in references	Average global Ni and Cu prices 2005–2015. Impacts not allocated to PGMs or Co because average coproduction levels orders of magnitude lower	Transport of intermediate and final products between mines and plants; transport of specific intermediate consumables: lime, sand, cement; diesel consumption for mining	Mine, processing and refining plants, machines, tailings disposal
	Class 1 Ni, produced hydrolateritically, converted into sulfate	Laterites	Open pit	Hydro	Sulfate crystallization add-on				
Cobalt sulfate	Co sulfate as an intermediate product				None	Mining: DRC (TFM Mine, Mutanda, Kamoto). Processing: DRC (TFM, Kamoto, Hanrui Cobalt project). Refined production: China (Tongxiang, Quzhou plants of Huayou Cobalt)	Average global copper and cobalt prices 2007–2016	Transport of intermediate ore product between mine, processing plants, and refining plants; diesel consumption for mining activities	Mine, processing and refining plants, mining trucks, tailings disposal
	Co produced as a metal, then refined into sulfate	Co–Cu ores (sulfides, oxides/laterites)	Underground and open pit	Hydro	Sulfate crystallization add-on				
Manganese sulfate	99.7% EMM with selenium via MnO	Carbonate, 19% grade	Open pit	Hydro (sulfuric acid leaching)	None; refinement excluded	China. Mining: Guangxi, Yunnan Provinces. Production: Ningxia Province	Direct allocation to manganese assumed	Transport of raw materials via road, transport of intermediate ore product	Buildings, roads, tailings disposal
	99.9% EMM no selenium	Carbonate, 44% grade							
	Non-battery grade from MnO concentrate		Underground (30%) and open pit (70%)	Pyro	None; refinement excluded	Mining data represent global averages including Asia and Australia. Processing data is not geography specific, as it is stoichiometrically based	Direct allocation to manganese assumed	Transport of intermediate ore between mine, processing plants, and refining plants; transport of intermediate products	Mine, processing and refining plants, tailings disposal
Non-battery grade byproduct of MnO ₂	Mn oxides								
Copper cathode	Hydro processing of lower-grade oxides	Oxide ores	Underground and open pit	Hydro	None	Numerous global locations aggregated by studies cited in references	Economic allocations based on economic value of Cu, Mo, and other coproducts; see source papers	Transport of intermediate ore product between mine, processing plants, and refining plants	Mine, processing and refining plants, tailings disposal
	Pyro processing of sulfides with molybdenum coproduct	Sulfide ores	Open pit	Pyro					

share, but more slowly for Class 1 nickel since the sulfidic source is the preferable format. A weighting of 85% pyrosulfidic in 2017, decreasing linearly to 60% by 2047, was applied. Since the literature used assesses the impact of pure nickel, an add-on process to produce nickel sulfate from Class 1 nickel metal was then modeled. This add-on consisted of incremental inputs only and assumed a

crystallization process using sulfuric acid and natural gas. The LCI for the add-on is included in Supplementary Data.

2.1.5.2. Cobalt sulfate. Cobalt is typically a low-volume byproduct of nickel or copper, and published LCA data on cobalt is somewhat limited. Ecoinvent includes an approximation based on 2000 data

of cobalt as a nickel byproduct, and (Farjana et al., 2019) produced a complete LCA analysis based primarily on this data. Two comprehensive primary data collection and LCA analyses were recently performed: one commissioned by the Cobalt Institute (CI) (Cobalt Institute, 2016), the other performed by Argonne National Laboratory (ANL) (Dai et al., 2018). Both leveraged recent literature, industry data, and company reports to compile LCIs representing current practices of the global cobalt industry. The CI study represents 30% of global refined cobalt production in 2012, but excludes Chinese production (60% of the global market) and does not provide granular stage data for the sulfate intermediate. The ANL study covers the three largest ore suppliers in the Democratic Republic of the Congo (DRC), where most of the world's cobalt is mined, and includes Chinese refineries. Most cobalt produced outside of China is currently produced to final metal form, while some Chinese producers create sulfate as an intermediate output, thus associating a premium with sulfates if produced outside of China; ANL's study includes both a direct cobalt sulfate production path as an intermediate, and the final cobalt metal LCI. Given its recency, geographic coverage, and production path coverage, this study was selected for the cobalt sulfate baseline. The paper's LCI data was input into SimaPro to generate the LCA results.

In the baseline, cobalt was therefore modeled as a byproduct of copper ore, mined in the DRC, and refined by plants in China using the Gecamines process. The anticipated exponential demand growth of cobalt sulfate was assumed to be primarily supplied by manufacturers making plant adjustments to output a more cost-effective and environmentally favorable cobalt sulfate intermediate (80%), while the remainder would be supplied by cobalt metal converted to sulfate using extra processing (20%). For the latter, a sulfate add-on process was modeled, following the same method as for nickel. Notably, the cobalt sulfate land-ore baseline assumed 100% hydropower for the DRC processing plants.

2.1.5.3. Manganese sulfate. Battery-grade manganese sulfate is commonly produced from one of two routes. The easier but costlier path is refining electrolytic manganese metal (EMM), a high-purity manganese predominantly produced in China. The technically harder route entails chemical refining of ore. Ecoinvent v3.5 includes two methods of making a lower-purity manganese sulfate (Levova, 2016a, 2016b), an intermediate step in the production of EMM and other manganese-derived materials. These data are based on a single German plant and may serve as an extreme lower bound, as they leave out substantial steps and material inputs needed to produce the battery-grade product. Two EMM LCAs also serve as conservative proxies for battery-grade sulfate. First, Peng et al. (2012)'s preliminary LCA of EMM, which notably excludes transport and infrastructure, highlights GWP's dependence on ore grade and electricity grid by comparing 99.9% purity EMM from high-grade ores in South Africa to 99.7% purity EMM created in China. Second and most recent, Zhang et al. (2020)'s robust LCA of EMM covers several Chinese regions and a large proportion of overall EMM production. Given China's dominance in EMM production and in battery-grade sulfate production, the Chinese EMM datasets received greater emphasis in the LCA baseline. EMM was assumed to represent 60% of battery-grade sulfate production, with 90% sourced from China. Non-Chinese EMM production was proxied by the South Africa results, an optimistic case with cleaner electricity and extremely high-grade manganese, while the ore route was proxied by the conservative Ecoinvent entries for non-refined, industrial-grade sulfate. Assuming accurate weightings, the overall result may be an underestimate of GWP, since final refinement material and energy inputs for battery-grade sulfate were not included, to the varying degrees noted.

2.1.5.4. Copper cathode. High-purity (99.99%) copper cathode is a typical format created by major copper-production pathways for commoditized sales. Numerous published studies have quantified the life cycle environmental impacts of copper, including Krauss et al. (1999), Norgate and Rankin (2000), Norgate, (2001), Ayres et al. (2002), Norgate and Lovel (2006), Norgate et al. (2007), Classen (2009), Norgate and Haque (2010), and Nuss and Eckelman (2014). Kuipers et al. (2018) more recently built on these: similarly to Verboon (2016), they augmented the Ecoinvent database with recent reports to produce a more up-to-date process baseline, then extended the results with future dynamics via an LCSA using the same United Nations Environment Programme (UNEP) and *World Energy Outlook (WEO)* supply scenarios as van der Voet et al. (2018) and Verboon (2016) for ore degradation and electricity-mix changes. Given the data recency, path robustness, and alignment to supply scenarios, Kuipers et al. (2018) was therefore deemed most relevant for this study's baseline.

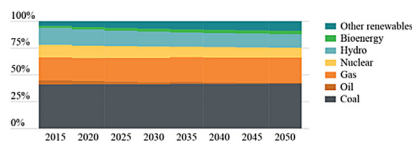
The two copper-processing routes, modeled following Kuipers et al. (2018), show oxides processed hydrometallurgically with a molybdenum coproduct, and sulfides processed pyrometallurgically with an anode slime byproduct. Following Kuipers et al.'s (2018) regression based on data from ICSG (2015), the initial path weight for hydrometallurgical processing was assumed to be 23% in 2017, and to grow linearly, reaching 30% by 2045.

2.1.6. Mass-based sensitivity analysis for land ores

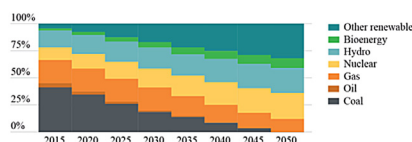
Mass-based sensitivity estimates for land-ore-based nickel sulfate and cobalt sulfate were taken from the source literature. Manganese sulfate and copper were conservatively estimated to take on the same values, based on the typical presence of no, few, or higher-value allocated coproducts. Detailed assumptions are provided in Supplementary Data.

2.1.7. LCSA supply scenarios for land ores

The two supply scenarios defined for land ores each contain up to three dynamic components: electricity-grid-mix shift, ore-grade decline, and energy-efficiency improvements. Electricity-mix scenarios were defined based on UNEP's Global Environmental Outlook (GEO)-4 and the International Energy Agency's (IEA) *WEO* scenarios, matching the scenarios modeled in van der Voet et al. (2018), Kuipers et al. (2018), and Verboon (2016). The baseline scenario was built on UNEP GEO-4 "Markets First" with its largely status quo economic growth policy drivers (UNEP, 2007), and *WEO*'s "Current Policies" electricity-mix scenarios (IEA, 2012), which show little renewables growth (Fig. 2). The green scenario was built on UNEP GEO-4 "Equitability First," with its equity-driven global policies, coupled with the aggressive renewable-electricity



(a) Baseline land-ores scenario, based on UNEP GEO-4 "Markets First" scenario and *WEO* "Current Policies."



(b) Green land-ores scenario, based on UNEP GEO-4 "Equitability First" scenario and *WEO* "450 Scenario."

Fig. 2. Background electricity mixes for two LCSA land-ores supply scenarios, 2015–2050.

policies of the WEO “450 Scenario” with coal-based electricity dropping to 0% by 2050.

For both electricity-mix scenarios, the anticipated ongoing impacts of nickel’s and copper’s declining ore grades were considered, with larger volumes of waste rock and ore required for the same final output and hence greater environmental impact, as modeled at different steps of the value chain by [van der Voet et al. \(2018\)](#), [Kuipers et al. \(2018\)](#), and [Verboon \(2016\)](#). In addition, [Kuipers et al. \(2018\)](#) showed that efficiency dynamics were significant and predictable for copper, and they mathematically quantified impacts for a subset of copper processes, based on an adaptation of the US Department of Energy “bandwidth method” to define a practical minimum that considers global average energy requirements, best practice requirements, and the theoretical minimum.

For nickel and copper, the published GWP time series results from the aforementioned sources, which incorporate electricity-mix scenarios, ore-grade declines, and energy-efficiency dynamics, were reused directly. For manganese and cobalt, background LCI electricity mixes were manually adjusted in a similar manner using SimaPro inventory outputs; the resultant GWP impact differences scaled the baseline. Direct production of industrial-grade manganese sulfate from Ecoinvent v3.5 ([Levova, 2016b](#)) was used as a proxy to obtain the scaling for manganese sulfate. All ore-grade time series, electricity-mix scenarios, and scenario results are provided in Supplementary Data.

2.1.8. Nodules model and foreground LCI data

2.1.8.1. Data sources and foreground LCI data. Although there are currently no commercial operational paths for processing and refining CCZ nodule metals, the inputs required for an LCA are available from robust studies and data resulting from efforts by CCZ contractors and the ISA. The LCA model aligns with the nodule collection, processing, and refining systems being developed by several ISA exploration contract holders (BGR/Germany, GSR/Belgium, India, NORI/Nauru) and draws on a data set developed by DeepGreen Metals and contained in the quality-controlled preliminary economic assessment compiled independently by [AMC Consultants \(2019b\)](#), with inputs including a technical CCZ resource statement compliant with Canadian standard NI-43-101, detailed engineering design artifacts, metallurgical plant design, results of polymetallic nodule metal-extraction pilot studies, and economic projections for the battery-grade metal formats.

The LCA model is based on a single operation collecting 4.9 metric Mt of dry nodules yearly, with product mass flows as shown in [Table 4](#). Price and market forecasting was performed by CRU International. For the offshore collection model, the operating parameters, equipment, material inputs, and emissions are based on nodule-collection system engineering by Deep Reach Technologies, Herbert Marine Engineering, and Cellula Robotics, with transport models by Pareto. Nodule shipping requirements are based on a

2000-kilometer (km), one-way trip with 60,000 metric tons of nodules cargo per trip. For the onshore processing and refining model, the flow sheet developed by Hatch dictated the material and energy inputs as well as emissions expected for each phase, which were directly input as foreground LCI. Other emissions contributions, e.g., transport-related emissions and indirect material impacts, were provided by the Ecoinvent-based background LCI. The nodule plant location is assumed to be proximal to a port as well as to hydropower. Through flow-sheet design choices, including material choice and recycling of residues, no tailings, residues, or solid waste for disposal are expected to be produced. Material inputs also reflect chemical-processing choices designed for lower life cycle emissions and reuse of byproducts. The complete nodules LCI is available in Supplementary Data.

2.1.8.2. LCA model. The LCA model for polymetallic nodules was designed with distinct modules to match the basic phases of nodule production: collection, processing, and refining. Included in the system boundary are use and maintenance of the collection system, port usage, nodule transfer by ship, conveyor belt transfer from port to processing plant, use of the plant, all materials and energy inputs, and transport of a subset of material inputs. The specific end products are nickel sulfate, cobalt sulfate, manganese sulfate (assumed as 5% of the manganese output, since the sulfate is a relatively small market), a 40% manganese silicate product as input to silicomanganese (SiMn) alloy production (the remaining 95%), and 99.9% pure copper, all located at the nodule-processing plant. Modeled byproducts are ammonium sulfate and a zero-net-value marketable converter slag ([Table 5](#)).

Allocation design ([Fig. 3](#)) was undertaken following ISO 14040/44. The process was subdivided into three allocation groups: (1) nodule collection, transport, and initial pyrometallurgical processing; (2) coal-based reduction, in which carbon binds with oxygen stoichiometrically and hence is physically allocated; and (3) hydrometallurgical refining of a polymetallic matte. Where physical basis of allocation was not possible, impacts were then allocated economically, and the mass-based allocation sensitivity was also calculated. The converter slag is an industrial input earmarked for sale for abrasives or road ballast, whose economic value is assumed to be offset by transport cost, and hence it receives zero allocation and is treated as an offsetting material credit. Final allocations are found in Supplementary Data. Although SiMn is not modeled as an end point in this LCA, the allocated impacts from producing the 40% Mn product stream are fully represented in the per kg impact assessment of the manganese sulfate output.

2.2. Carbon sequestration impact estimation methods

2.2.1. Land ores

Mining can interact with the carbon-sequestration process

Table 4

Mass flows and values of CCZ nodule product streams for an operation processing 4.9 metric Mt of dry nodules yearly. Mass flows are based on the preliminary economic assessment for CCZ NORI Area D, independently compiled and signed off by [AMC Consultants \(2019b\)](#). Prices are projected averages from 2025 to 2055 given per metal amount in final-product forms.

Mass item	Annual flow (metric tons)	Average value (USD per metric ton)
Wet nodules collected at offshore vessel	6,400,000	
Dry nodules at processing facility	4,880,000	
Nickel contained in sulfate	60,700	19,926
Cobalt contained in sulfate	6000	51,007
Manganese contained in Mn silicate product	1,383,000	390
Copper cathode	48,700	7084
Ammonium sulfate	171,000	90
Converter slag	509,000	0

Table 5
Nodules model summary.

Pathway description	Ore type	Mine type	Process type	Geographies	Price data for allocation	Transportation included	Infrastructure included
Nickel sulfate	Polymetallic nodules	Deep-sea collection	Pyrometallic processing, hydrometallic refinery	CCZ collection with North American Pacific coastal processing plant	Projected average prices 2025–2055 by CRU International of nickel and cobalt in sulfate, copper cathode, and manganese in 40% grade product	Transport of nodules from collector to plant via ship and conveyor; transport of specific intermediate consumables: coal, sulfur, sulfuric acid, Mn sulfate refinement materials	Production vessel, transport vessels, processing plant, machines
Cobalt sulfate							
40.2% manganese silicate product							
Manganese sulfate							
99.9% refined copper							
Ammonium sulfate							
Converter slag							

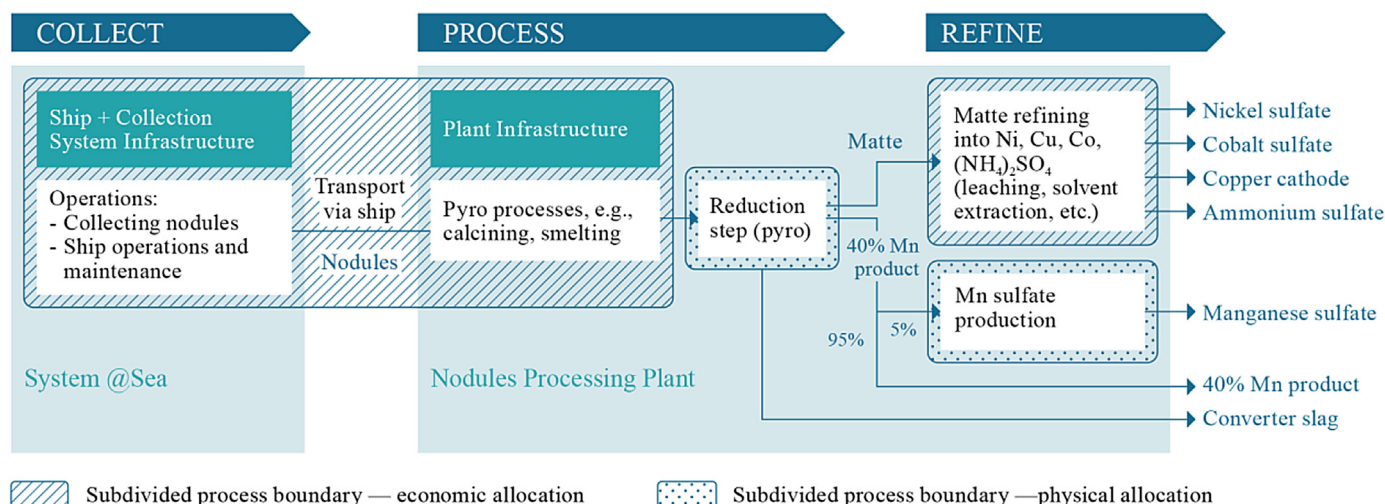


Fig. 3. Nodule operations product flow and allocation schematic.

through two primary mechanisms: land transformation and pollution. First, some of the sequestered carbon is released when forests, vegetation, and soils are removed for the mines and processing plants. Carbon can also be released when the land is debilitated by contamination with toxic water, dusts, and air emissions. Second, physical damage and contamination may impede revegetation of habitats, which reduces the future capability for the ecosystem to sequester carbon. Habitat damage may happen through land and water contamination, land use for tailings dams, tailings dam collapses, and other mechanisms. The damage to carbon sequestration caused by terrestrial mining varies by mine type, location, size, mining methods, and local habitats and ecosystem characteristics. The total area of damage typically far exceeds the geographical area of the mine site as a result of water and air pollution, construction of access infrastructure and miners' accommodations, and other impacts of mining communities. No estimates of the overall impact of the mining sector or impacts of individual mines on carbon sequestration were found in published literature. An estimate was therefore constructed of the amount of sequestered carbon at risk of release from clearing vegetation and soil for the land footprint of terrestrial mining.

This estimate began with a literature review to determine the stored carbon per unit area in soil and vegetation. An average was

used across biomes. While stored carbon density can be highly variable, the spectrum of land types involved in mining these four metals includes highly biodiverse areas, particularly as noted for nickel. Next, the land-ore LCA baseline was used to compute the "land competition" indicator from the Institute of Environmental Sciences (CML) LCIA standard. This is roughly representative of terrestrial land area used to produce each kg of metal from land ores, including both direct and indirect life cycle contributions. For nickel and copper, these per kg land competition values were converted to a time series incorporating ore-grade decline: the ore-grade time series was applied, with an assumption that 40% of land-use impact varies directly with the volume mined (inversely with grade). For each metal, the resultant time series of per kg land use (or static values for cobalt and manganese) was combined with the average stored carbon estimates above, giving a time series of potential carbon release per kg of metal produced. An additional check was performed separating forested and non-forested biomes. Combining the carbon-release time series with Morgan Stanley's metal-demand time series yielded the total amount of sequestered carbon at risk from producing metals for 1 billion EVs from land ores.

Separately, the potential disruption to future carbon-sequestration services was estimated. Open pit mines, infrastructure, roads, and other land uses can lead to medium- or long-term disruptions of

sequestration services, particularly when mine sites are abandoned without remediation (millions of mines are estimated to be abandoned globally). The analysis assessed the impact of complete removal of sequestration services from all affected soil and vegetation for 1 billion EVs for 100 years, after which time sequestration services were assumed to be fully restored.

2.2.2. Deep-sea nodules

Three different mechanisms were examined to understand the potential release of sequestered carbon when producing metal from nodules: seabed disruption during nodule collection, carbon release from riser water during surface operations, and terrestrial disruption from the land footprint including onshore processing. First, nodule collection will temporarily suspend deep-sea sediments that store carbon. Estimating the total carbon at risk in impacted deep-sea sediments required considering the size of the seabed disturbed by nodule collection, the density of carbon content within the seabed sediment, and pathways for stored carbon to physically rise to the ocean surface and enter the atmosphere. A literature review coupled with chemical sampling data from the NORI Area D site in the CCZ produced an estimated range of stored carbon per disrupted area in the CCZ deep seabed. The disrupted seabed area for 1 billion EVs was calculated using average nodule metal densities in the CCZ. Combining these two inputs yielded an upper limit for sequestered carbon at risk under this mechanism. The upper limit was refined into an estimate based on the current understanding of pathways for disturbed carbon to rise from the deep seafloor and into the atmosphere.

The second mechanism, carbon release from riser seawater, will be activated when the deep seawater used to lift nodules from the deep seabed to the ocean surface is briefly exposed to air in a decompressed setting. These large volumes of seawater are sourced from below the carbonate compensation depth, where solid carbonate is dissolved into the seawater under pressure. In being brought to the surface, the slightly warmed, depressurized seawater is likely to be exposed to expanding compressed air inside the riser pipe for 545 s, and to ambient surface air in the hold of the surface-production vessel for 300 s. During these times some CO₂ may be released before the water is returned to the deep ocean. The maximum CO₂ directly exchanged with the atmosphere during that exposure was calculated as shown in equation (1). Allocating this to the metal outputs and scaling to 1 billion EVs yielded the second result for nodules.

Maximum CO₂ released per year per nodules operation = water mass pumped [Mt water / year] x change in dissolved inorganic carbon [mole CO₂ / Mt water] x 0.044 kg / mole CO₂ (1)

Third, while nodule collection occurs offshore, onshore processing plants have physical land footprints which contribute first-order impacts, and offshore energy and equipment use contributes second-order impacts. The land competition LCIA indicator was therefore also estimated for each nodules-based metal, then scaled to metal quantities required for 1 billion EVs, arriving at the third result for nodules.

Separately, the potential disruption to future carbon-sequestration services was again estimated. Similar to the disruption of carbon-sequestration services on land, mechanisms for sequestration-service disruption from nodule collection were examined in the scenario whereby these services cease completely for 100 years and resume thereafter. Nodule collection's land-based contribution to carbon-sequestration service disruption was then also calculated, based on its LCIA-derived land footprint and using the same procedure as with land ores.

3. Results and discussion

3.1. GWP assessment results

3.1.1. Land ores versus nodules comparison (per kg GWP)

Cradle-to-gate GWP results for the land-ore baseline and the nodules model are seen in Fig. 4. Under either allocation method, all four metals generate significantly less CO₂e when produced from nodules. Of the four, higher-impact nickel sulfate and copper represent the bulk of per EV metal mass and also show the greatest relative per kg difference between land ores and nodules. In addition, the byproduct ammonium sulfate, commonly used as a high-nitrogen soil fertilizer, shows a low GWP of 0.02 kg CO₂e per kg, in part due to its relatively negligible market value compared to the metals. Nodules are thus effectively a source of near-zero-emission, fertilizer-grade ammonium sulfate byproduct, as conventional sources can range from 0.4 kg CO₂e (Ecoinvent, 2018) to 2.0 kg CO₂e (Heil, 2018) per kg of ammonium sulfate. Under the mass-based sensitivity analysis for nodules, ammonium sulfate's GWP rises by 40x to 0.7 kg CO₂e and manganese sulfate's GWP rises slightly, while the other three metals' emissions drop between 49% and 93%. The lower per kg GWP of nodules is robust under both allocation methods.

The GWP of the nodules-based 40% manganese silicate product, an intermediate product to manganese sulfate and of high value to SiMn producers, is estimated at 1.25 kg CO₂e per kg of manganese. As the bulk of this product is likely to be used in the production of an alloy such as SiMn, a useful follow-on study once the LCI is available would be to compare the GWP of the nodules-based SiMn alloy to a land-ores-based product. A strong candidate for the latter is the recent robust study commissioned by the International Manganese Institute and conducted by Hatch, augmenting the Ecoinvent and GaBi databases with extensive primary data to create the first global LCA of manganese-alloy production, covering 16 producers worldwide and 18% of 2010 global manganese production (Westfall et al., 2016; Hatch, 2014).

3.1.2. GWP breakdown by phase for nodules

To help understand the drivers behind the nodules-based GWP, one can examine the GWP of producing metals from 1 kg of nodule broken down by collection, processing, and refining phases (Fig. 5). Less than 10% of GWP is due to offshore collection and transport, including the infrastructure, fuels, and operations. These offshore results are close to Heinrich et al.'s (2020) offshore nodules GWP reported for the scenario based on Romboll IMS HWWI (2016), which exploits a low-energy design reportedly in line with industry expectations for energy use for this scale of nodule collection. The nodule results contrast to land ores, for which roughly half of emissions may come from mining and concentration phases, as illustrated in Nuss and Eckelman (2014).

The reasons for nodules' lower GWP results include their relatively low-energy-intensity collection phase, high ore grades (no concentration step required), and ocean location enabling low-footprint, ship-based transport to the onshore plant. The relatively large GWP seen in nodules' pyrometallurgical processing phase is driven by coal-intensive reduction of oxides in the nodules; the reduction step alone contributes nearly three-quarters of the cradle-to-gate CO₂e per kg of nodule processed, making it a prime candidate for innovations that could reduce GWP (e.g., use of low-carbon reductants).

GWP is sensitive to electricity source, and electricity can become one of the largest contributors to GWP if there is heavy use of fossil fuels in electricity grids. Nodules' high energy requirements for reduction are countered by the low impacts of hydropower. For instance, a low GWP is seen in the refining phase, despite the

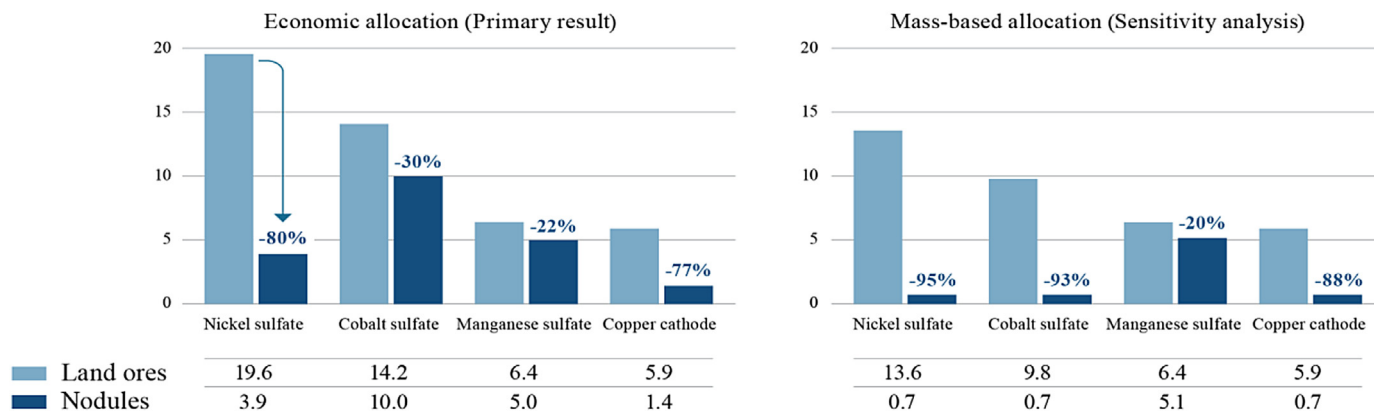


Fig. 4. Cradle-to-gate emissions comparison, land ores versus nodules (kg CO₂e per kg metal).

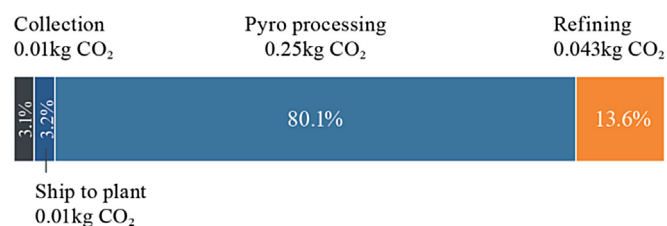


Fig. 5. 0.313 kg CO₂e released to produce metals from 1 kg of wet nodule.

electricity requirements for copper electrowinning. The dominance of hydropower in land ores' cobalt processing may partially suppress its GWP as well, as a full global average would include non-DRC plants that may not use hydropower. Land-based mining often requires metallurgical plants to be located close to mines, as low-grade metal ores, with their relatively high mass and low value, cannot be economically shipped over long distances. This constrains electricity inputs to local grids and frequently drives up environmental impacts, wastes, and GWP. Nodule collectors' flexibility in placing metallurgical plants anywhere near a deep-water port allows flexible access to hydropower or other renewables and to byproduct end markets, structurally providing an environmental advantage to be leveraged.

3.1.3. Static land-ore baseline versus nodules (1 billion EVs)

Scaling the as-is, per kg GWP results to the total metal needed for 1 billion EVs yields a total static GWP value for each source: 1749 metric Mt CO₂e for metals produced from land ores versus 445 metric Mt CO₂e from nodules (Fig. 6), or a 1.3 metric Gt (−75%)

reduction. A mass-based sensitivity analysis shows lower GWPs for both sources and roughly the same absolute differential—1379 metric Mt CO₂e for land ores and 139 metric Mt CO₂e for nodules, or a 1.2 metric Gt (−90%) reduction (Fig. 7). Note that this static case assumes present-day ore grades, mineralogies, electricity mix, energy densities, and production path weights.

3.1.4. Baseline land-ores scenario versus nodules

Next, to understand how GWP may change with time, dynamic LCSA results are examined. In the baseline scenario for land ores, assuming status quo global policy trends, the negative impacts of falling ore grades worsen the land GWP result. In comparison with the static values given above, per kg GWPs for land-ore-based nickel sulfate and copper cathode under the baseline dynamic scenario increase by 8% and 14% respectively by 2047. As a result, the overall GWP to produce battery metals and connectors for 1 billion EVs increases by 6% or 0.1 metric Gt CO₂e to 1850 metric Mt CO₂e. Examining the total results from both sources (Fig. 8), the GWP of producing metals for 1 billion EVs is 76% lower using nodules (91% lower with mass-based allocation) compared to land ores under the baseline dynamic scenario.

3.1.5. Green land-ores scenario versus nodules

The green scenario for land ores envisions an aggressive transition away from fossil fuels in the electricity mix time series, with coal decreasing from 41% of electricity grid makeup in 2015 to 0% in 2050. This scenario materially and positively impacts GWP projections for land ores. Unlike in the baseline scenario, electricity-mix benefits are several times larger than the negative impacts of ore-grade declines. GWP values for individual metals in the baseline decrease between −19% and −35% by 2047, with nickel seeing

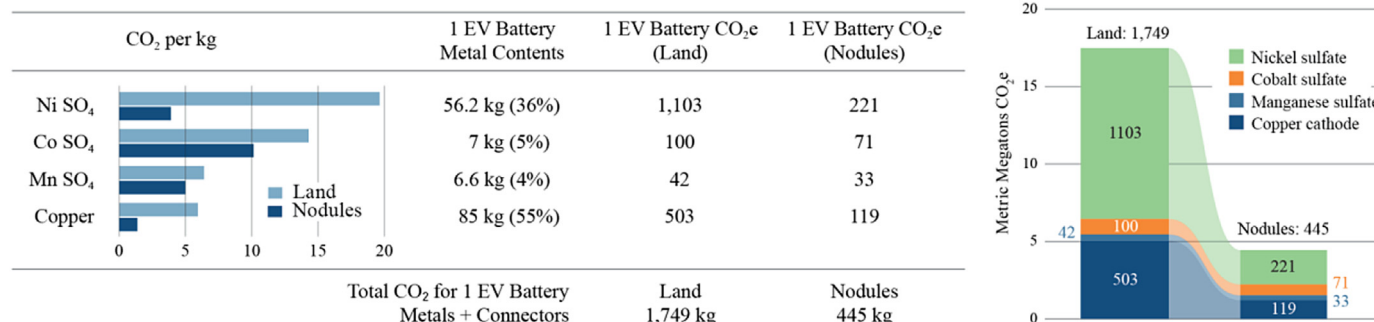


Fig. 6. Static GWP results (kg CO₂e) for as-is land ores versus deep-sea nodules—economic allocation.

CO ₂ per kg	1 EV Battery Metal Contents	1 EV Battery CO ₂ e (Land)	1 EV Battery CO ₂ e (Nodules)
Ni SO ₄	56.2 kg (36%)	764	40
Co SO ₄	7 kg (5%)	69	5
Mn SO ₄	6.6 kg (4%)	42	34
Copper	85 kg (55%)	503	60
Total CO ₂ for 1 EV Battery Metals + Connectors		Land: 1,379 kg	Nodules: 139 kg

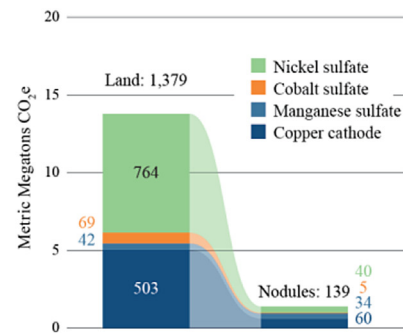


Fig. 7. Static GWP results (kg CO₂e) for as-is land ores versus deep-sea nodules—mass-based allocation sensitivity test.

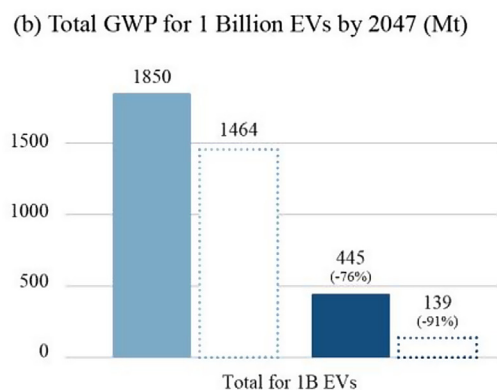
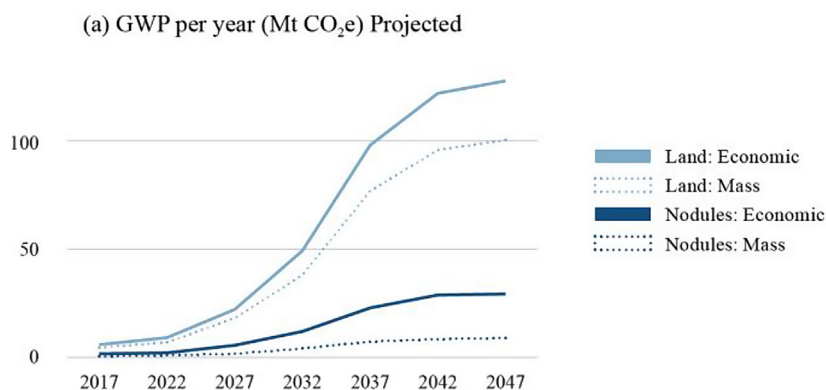


Fig. 8. Dynamic LCSA GWP results (metric Mt CO₂e)—baseline land-ores scenario versus nodules.

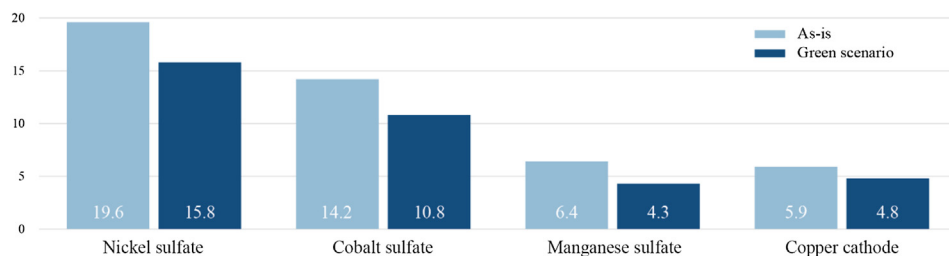


Fig. 9. Land-ores-based GWP improvement (kg CO₂e) under green scenario. Shown are per kg GWP values for land ores, comparing 2017 as-is values with final 2047 green land-ores-scenario values.

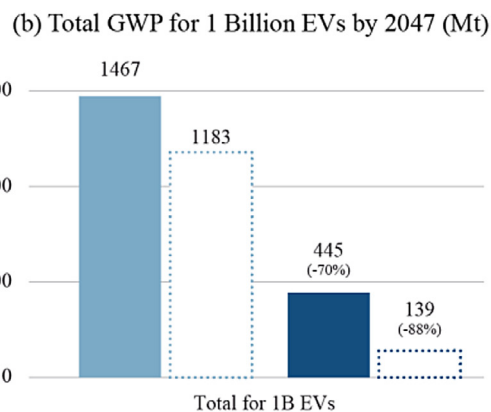
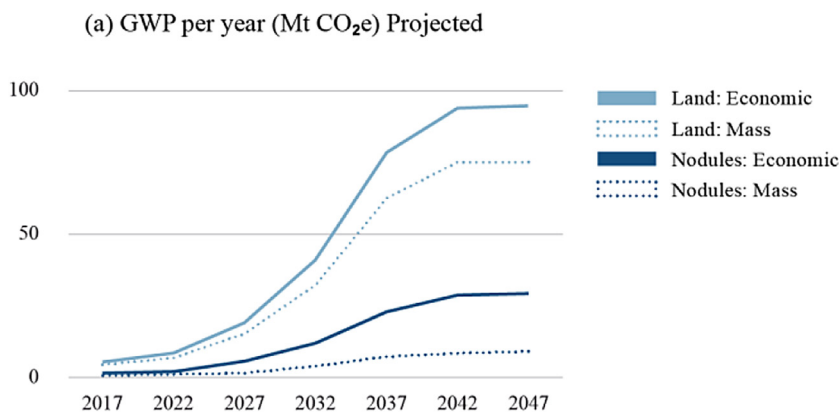


Fig. 10. Dynamic LCSA GWP results (metric Mt CO₂e)—green land-ores scenario versus nodules.

the greatest absolute impact improvement (Fig. 9). Even with this benefit, the GWP for producing metals for 1 billion EVs is still 70% lower using nodules (88% lower with mass-based allocation) compared to land ores under the green dynamic scenario (Fig. 10).

3.1.6. Uncertainties in nodule results

There are several sources of potential variability in the nodule results. First, technological and operational design choices in the offshore collection stage may affect GWP, such as collector design, collection processes, and bulk transport vessel processes. Energy intensity and energy source (e.g., fuel type) used in offshore production are expected to be key drivers of variability. Instead of using the conventional marine fuels assumed in this paper, operators could elect to power offshore production with electrofuels (e.g., ammonia produced using renewables), thereby dramatically reducing the GWP of offshore operations. While some variability in the offshore stage is anticipated, as examined in Heinrich et al. (2020), the climate change impact of this stage is expected to be small compared to onshore processing, as illustrated in Fig. 5. Second, metallurgical design choices determine precise material and energy requirements: macroscopically, the choice of a hydro-metallurgical or pyrometallurgical strategy can imply greater GWP-impacting material or electricity requirements; microscopically, final, detailed flow-sheet design and equipment can further drive variability. This paper assumes a coal-intensive pyrometallurgical processing (with coal use accounting for ~80% of the stage impacts) with hydrometallurgical refining, and a flow sheet designed to produce zero solid waste. Less energy-intensive processing pathways are possible (e.g., Cuprion, high-pressure acid leaching) and would likely produce significantly lower GWP results. However, these pathways also produce toxic tailings, leading to expanded land use (higher disruption of carbon-sequestration services) and the environmental requirement to manage tailings indefinitely. Third, strategic choices relating to plant location and material sourcing can directly and indirectly affect transport distances and electricity mix, and hence GWP. Fourth, moving from design and lab-scale tests to large-scale pilot and commercial-scale plants will likely result in GWP reductions from further flow-sheet optimizations and from the reduction or replacement of carbon-rich consumables. Studies by Hatch show that coal use could be reduced by as much as 20%, or coal could be altogether replaced with biochar or renewable hydrogen; either would lead to a dramatic reduction of the GWP of the processing phase. Model assumptions (e.g., distances, material and energy quantities, yields) can also increase in precision as the system moves into commercial production. Fifth, the LCA process relies on background data, which are proxies by nature; small impact deviations are characteristic of any LCA model as it leverages approximations built into the background database.

Results were therefore stress tested for sensitivities to specific Ecoinvent item variants, foreground data geographies, and database versions. In most cases, outcomes under tests varied by less than 1–2%. Any components, materials, or phases involving operator choice and contributing high GWP sensitivity were assessed. Two important sensitivities were identified: foreground electricity mix and ship transport distance (both driven by plant location). On the former, a substantial GWP increase based on the proportion of operators not using a renewable electricity source is to be expected. On the latter, shipping distances may deviate from the assumed 2000-km one-way trip. In Heinrich et al.'s (2020) offshore study, key potential plant sites were located in Mexico (~1700 km), Canada (~3700 km), and Cuba (~5100 km). As ship transport contributed 3% of GWP per kg of nodule in the present study, if plants are located twice or three times as far, GWP would rise by 3% and 6% respectively. Additionally, if nodules received the same dynamic background-electricity-mix improvements as the green land-ores

supply scenario, a further reduction of GWP would be seen. Since only background electricity inputs change under this treatment, use of hydropower for processing and refining is unaffected. Improvements of similar order as land ores' green versus baseline scenario differences may be expected, i.e., –22% to –32% metal-specific, per kg GWP reductions in year 2047, or around –21% cumulative reduction for 1 billion EVs.

3.1.7. Uncertainties in land-ore baseline

Uncertainty in the land-ore baseline manifests as four potential deviation types: (1) accuracy of the selected production paths in representing actual global contribution volumes for these specific battery metals; (2) uncertainty in future weights for each included production path (e.g., how will the percentage of Class 1 nickel coming from laterites versus sulfides change over time?); (3) static uncertainties arising from data quality of referenced literature and of LCI add-ons; and (4) future uncertainties of two varieties—deviations from the specified time-series scenarios (i.e., ore grade, electricity mix, and energy efficiency), and GWP improvements in land-ore averages via retrofits and new projects. Many of the above uncertainties can nudge the answer in either direction.

To address the first, emphasis was placed on selecting production paths relevant to producing battery-grade metals in the proper format, using high-quality data. Rationale of selections and potential deviations, such as the noted deviations for manganese, have been mentioned and are further expanded upon in Supplementary Data. For the second, while literature informed weight selections, some assumptions about future production line shifts were necessary. Sensitivity tests were performed on the weights, allowing a –30% relative weight reduction on the dominant path for each metal, or an increase of half its distance to 100%. This yielded individual GWP deviations of –13% to +4% (nickel), –11% to +26% (cobalt), –18% to +25% (manganese), and –4% to +8% (copper), aggregating to a total GWP deviation range of –9% to +13% (1 billion EVs in the static case). For the third, uncertainties provided by individual data sources are noted in Supplementary Data and available in referenced literature. LCA data is also inherently time lagged; quantified production process measurements are often years behind current practices, so recent process improvements are often not reflected. For the fourth, it is certainly likely that the future will deviate from either scenario studied. A scenario approach allowed for assessment of a range of possible futures and understanding of a relative magnitude range. Reducing fossil fuel usage to 0% by 2050 seems unlikely, but individual operations may improve environmental practices in tandem.

3.1.8. Interpretation

The differences seen between land-based and nodule-based GWP results seem substantial and were robust to sensitivity analyses performed on the nodules model, Ecoinvent database version, land-ore path weights, and LCA allocation method. The green land-ores scenario considered a future in which aggressive improvements have been made on a global scale, but the likely reality is probably somewhere between the two scenarios. While the nodules model assumed use of hydropower, future improvements in background electricity mix were excluded, and these opposing assumptions may have effects of similar scale. As more operation instances are designed and operationalized, additional nodule pathways can be modeled to deepen the literature, and the present model may be refined once operational data become available. Qualitative conclusions are not expected to change; notably, any non-pyrometallurgy-based nodule paths exclude the largest emissions driver seen in this study: coal-based reduction.

In the future, land-ore and nodule operations are anticipated to adopt initiatives that reduce their respective GWP footprints. The

nodule-mining industry is still in the exploration phase, and further efficiencies are likely to be captured once it moves into commercial production. Significant GWP reduction could be achieved if carbon-neutral or carbon-negative alternatives to coal are considered, as coal-based reduction drives much of the nodules' impact when the pyrometallurgical route is used. On land, global pressures continually incentivize land-ore operations to invest in environmental improvements. Realistically, such improvements, along with unpredictable disruptive process innovations, take extended periods and massive efforts to roll out on a global scale; as [Hein et al. \(2020\)](#) note, it is far easier to adopt environmental best practices with a new beginning than by retrofitting a massive global industry. GWP may also further improve if new ore deposits with substantially higher grades are discovered and exploited (although this would not negate any negative ecological habitat and social impacts); however, such discoveries are unpredictable, and the ore-grade decline trend has been decades long without indication of a likely change of course. Nodules furthermore have a structural environmental advantage since four high-grade metals are found together in one ore and no toxic levels of heavy metals are present. To produce the same final metal amounts using land ores, three different ores of lower and/or falling grades are needed, and a much larger overall mass of ore is exploited for the same metal output, often accompanied by the need to manage toxic waste. Even under an ideal scenario of industry-wide optimization of land-ore mining and processing practices, these factors place an innate upward pressure on impact.

3.2. Carbon sequestration results

3.2.1. Impact from land ores

3.2.1.1. Release of sequestered carbon. An average terrestrial organic carbon content of 16,200 metric tons per square km (km^2) was calculated as the average of three estimation methods: (1) biome-by-biome estimates from [Trumper et al. \(2009\)](#); (2) vegetation, soil, and detritus organic carbon estimates by [World Ocean Review \(2010\)](#); and (3) soil estimates by [Zomer et al. \(2017\)](#) plus vegetation estimates by [Erb et al. \(2018\)](#), [Lal \(2004\)](#), and [FAO \(2010\)](#). In all cases, land area used was the total land area of earth, $1.49\text{E}+08$ ([Wikipedia, 2019](#)), minus 10% covered by glaciers and ice caps ([National Snow and Ice Data Center, 2020](#)), equaling $1.34\text{E}+08 \text{ km}^2$. Next, using the land-ore baseline, the land competition indicator—including direct impacts from mine sites, processing and refining sites, and roads, as well as indirect life cycle impacts from material and energy use—was estimated at $156,000 \text{ km}^2$ to produce the metals for 1 billion EVs by 2047, including the effects of ore-grade dynamics. Multiplying this average carbon content by the land ores' land requirement yielded 2.53 metric Gt of stored carbon at risk. When exposed to air, oxidation plus microbial metabolism can eventually convert that carbon to 9.3 metric Gt of CO_2 . This is the estimated maximal risk for release of sequestered carbon associated with metal production from land ores. Mining risk to sequestered carbon on land can be somewhat reduced if mines separate out and protect from the air some portion of the removed soil or cut vegetation, through methods like stacking or burial. Note that estimates of sequestered carbon may refer to different soil depths ([FAO, 2010](#)). On land, depth can be to 1 m, and terrestrial mining typically removes at least that amount.

3.2.1.2. Disruption of future carbon-sequestration services. [Lu et al. \(2015\)](#) estimated the total net annual carbon-sequestration rate for land ecosystems of the coterminous US to be 323 metric Mt per year from 2001 to 2005, with forests contributing 97%. Given a forested area of 3 million km^2 and non-forested area of 4.65 million km^2 across the coterminous US, this yields an average of 104 metric

tons of carbon/ km^2 per year in forested areas and 2.1 metric tons of carbon/ km^2 per year in non-forested areas. With $65,700 \text{ km}^2$ of forest and $90,400 \text{ km}^2$ of non-forest comprising the $156,000 \text{ km}^2$ LCIA land area to produce metals for 1 billion EVs from land ores, the total carbon that could have been sequestered over 100 years had mining not occurred would be 0.7 Gt of carbon, equivalent to 2.6 Gt of CO_2 . Looking globally, though not differentiating by terrain type, [Keenan and Williams \(2018\)](#) estimated annual global terrestrial carbon sequestration to be 3.61 metric Gt. Dividing this by the global ice-free land area, 134 million km^2 , yields an average of 27 metric tons of carbon/ km^2 sequestered yearly. Applying this evenly to the $156,000 \text{ km}^2$ land area impacted by terrestrial mining for 1 billion EVs gives 0.42 metric Gt of carbon that could have been sequestered over 100 years had mining not occurred, or 1.5 metric Gt of CO_2 . The average of the two estimates is 0.56 metric Gt of carbon, or 2.1 metric Gt of CO_2 . Note that, in Amazonian Brazil, secondary forests around 60 years old contain just over 41% of the average carbon compared to the nearest primary forests ([Elias et al., 2020](#)). This regrowth data suggests that 100 years may be a reasonable time frame for estimating the disruption of carbon-sequestration services.

3.2.2. Impact from nodules

3.2.2.1. Release of sequestered carbon. The total sequestered carbon at risk from three mechanisms considered for polymetallic nodules is less than 0.6 metric Gt of CO_2 for 1 billion EVs. Impacts from the three mechanisms are described below.

3.2.2.1.1. Mechanism 1: Seabed disruption. The seabed footprint from nodule collection for producing metals for 1 billion EVs is calculated at $508,000 \text{ km}^2$, allocating economically the metal requirements as with the land estimate. Calculations assume an average of 15 metric tons of wet nodules per km^2 in the CCZ, metal concentrations as surveyed by [AMC Consultants \(2019a\)](#), 85% collector pickup efficiency in collection areas, and 15% of nodule fields set aside by individual operators as no-take zones. Although the disrupted seabed area is more than three times larger than the land area disrupted by metal production from land ores, the total carbon at risk is lower because carbon concentrations in CCZ sediments are on average at least an order of magnitude lower than in terrestrial soil.

Despite its vast area, the global seabed surface contains up to 15 times less carbon than all vegetation and soil on land. Data from [World Ocean Review \(2010\)](#) indicates that, globally, 150 metric Gt of carbon are stored in 354 million km^2 of seabed surface (424 metric tons/ km^2), while 2300 metric Gt of carbon are stored in 130 million km^2 of vegetation, soil, and detritus on land ($17,700$ metric tons/ km^2). [Ciais et al. \(2013\)](#) state a higher total value of 1750 metric Gt for marine surface sediments, yielding a global average of 4940 metric tons/ km^2 , still much lower than the average value for land. Estimates of seafloor carbon are typically for 10–30 cm, slightly higher than levels that could be disturbed during nodule collection (currently expected at 10 cm or less). DeepGreen engineers anticipate disturbance of only 5 cm of sediment underlying the nodule layer; at best, analyzing 10 cm of sediment depth overstates the amount of carbon disturbance expected and follows a precautionary approach. The lower quantity of carbon in surface sediments occurs in part because most carbon is metabolized in the water column before it reaches the bottom, as microbes decompose particles during their long voyage downward. As a result, the amount of organic carbon stored per area within the top 10 cm of CCZ abyssal sediments is far less than in terrestrial soil.

The percentage of carbon contained in CCZ sediment ranges from 0.2% to 0.6% by weight, decreasing with depth and remaining constant below 30 cm at <0.2% ([Volz et al., 2018](#)). Sediment samples from the CCZ NORI Area D seafloor area averaged 1.17 g/cm^3 wet

weight; 0.31 g/cm³ dry weight; 0.49% carbon; and 151.9 g of total organic carbon per square meter (151.9 metric tons/km²). In contrast, soil carbon values in the Unified North American Soil Map range from 0.87% to 51% (Liu et al., 2013). The median value for soil, 17%, is more than 300 times higher than for CCZ sediments. Scaling this to the 508,000 km² of allocated CCZ seafloor area to produce metals for 1 billion EV batteries and connectors, disturbed to a depth of 10 cm, the total sediment displaced would be 59.5 Gt wet (15.8 Gt dry) and would contain 0.08 Gt of carbon.

Almost none of this 0.08 Gt of carbon sequestered in seabed sediments suspended at 4–6 km depth can reach the sea surface and the atmosphere. When sediments are disturbed, resulting plumes are expected to rise no more than 100–200 m from the seafloor, and 99% of the suspended material is expected to resettle back to the bottom within one to two months and within 1–100 km (Jones et al., 2017). If the residual 1% were to remain afloat indefinitely, it could reach the surface and potentially the atmosphere after decades or centuries of thermohaline circulation. The maximum amount of carbon at risk of release is less than 1% of 0.08 metric Gt (less than 0.0008 metric Gt) of carbon, equivalent to <2.8 metric Mt of CO₂, for 1 billion EVs.

Depending on the efficiency of sediment separation from nodules in the seabed collection machine, small amounts of entrained sediment may rise along with nodules and water to the surface, then be discharged along with discharge water below the mixing depth. These particles may move laterally with currents while slowly sinking. While resettlement of such discharged sediment would take longer, a similar conclusion applies and 99% is expected to resettle over some timescale, albeit over a larger area, not affecting the quantity of carbon at risk of release.

In sum, because seafloor carbon density is low, and because the carbon has no known pathway for reaching the atmosphere other than the ocean's thermohaline circulation (centuries timescale) or earth's geological cycle (tens or hundreds of millions of years), nodule collection is not expected to release significant amounts of carbon sequestered in seabed sediments.

Responding to concerns (from, e.g. Greenpeace, 2019, and Howard et al., 2020) that DSM could harm the global climate by releasing carbon stored by the seafloor, an additional investigation was undertaken to assess whether nodule collection on the CCZ seafloor risks disturbing reservoirs of liquid or clathrate methane or CO₂. This appears unlikely. First, cold temperatures (~1.5 °C) and intense ambient pressure in CCZ sediments (5700–8500 psi at mining depth of 4000–6000 m) would keep such reservoirs intact in liquid or solid form (see phase diagram in Fig. 1 of Girotra et al., 2012). Second, the specific conditions in the CCZ are not associated with the formation of such reservoirs, and no such reservoirs have been found in the CCZ to date. Methane clathrates are typically found in shallow-water sediments and under permafrost in polar regions, and in deeper sediments along the margins of highly productive continental slopes (USGS n.d.). Processes by which they form are described by You et al. (2019) and typically require anaerobic bacterial decomposition of organic matter. Surface waters overlying the CCZ seabed are nutrient poor with low primary production, so insufficient amounts of organic matter reach the bottom to support large accumulations of methane. Furthermore, surface sediments are fine-grain clay, which typically supports only diffuse and dilute clathrate formation (You et al., 2019). Finally, CCZ sediments are oxic to at least 2 m, so any methane clathrate that did form would be below that level and would not be disturbed by nodule collection, which is limited to the top 10 cm. Both methane and carbon dioxide clathrates are also found in association with hydrothermal vents and cold seeps (Hester and Brewer, 2009; Levin et al., 2016), which are not known to occur in the CCZ. Therefore, it seems very unlikely that either methane or carbon dioxide

clathrate reservoirs occur in the CCZ or would be disturbed by nodule collection there.

3.2.2.1.2. Mechanism 2: Riser water. The second possible pathway of release of previously sequestered carbon arises from cold, pressurized seawater being pumped to the surface. To lift nodules to the surface, large volumes of seawater are sourced from below the carbonate compensation depth, where solid carbonate is dissolved into seawater under pressure. During its trip to the surface, deep seawater gets depressurized and warmed, and could release some CO₂ to the atmosphere while exposed to air bubbles for 545 s or less during the final 2500 m of ascent, and then to ambient air for another 300 s in the hold of the surface-production vessel.

Airlift raises approximately five times as much water as nodule mass; lifting 6.4 million metric tons of wet nodules per year would require ~32 million cubic meters of deep seawater. Under the extreme case where the deep seawater is fully equilibrated with present-day atmospheric CO₂, the resulting dissolved inorganic carbon quantity becomes ~2220 μmol/kg, or a change of ~120 μmol/kg. This assumes deep tropical water (0–20°N, ~4 °C) containing dissolved inorganic carbon of ~2340 μmol/kg, alkalinity of ~2380 μmol/kg seawater, and surface water containing an estimated pCO₂ of ~910 μatm, or 985 μatm if the water warms from 1 °C to 6 °C during its upward passage and brief stay within the hold of the surface ship. Assuming a pumping rate of ~1 cubic meter per second, the maximum annual CO₂ release to the atmosphere would be 3.84 × 10⁶ mol CO₂ or 170 metric tons of CO₂ for a 6.4 million wet metric ton operation per year. This translates to about 27 g of CO₂ release into the atmosphere per wet metric ton of nodules. Allocating this release economically and scaling up to 1 billion EVs yields a total maximum release of 0.00015 Gt of CO₂ from riser water. To put this number into context, nodules' potential carbon-sequestration impact via this method is less than 0.1% of the total life cycle CO₂e emissions discussed earlier in the section on GWP.

The realistic release to the atmosphere would likely be much lower because the kinetics of gas/water exchange are slow. Only a negligible amount of the dissolved inorganic carbon is in the form of aqueous CO₂ gas that can be directly exchanged between water and air. Because of this, CO₂ gas exchange is roughly an order of magnitude slower than that of other gases like O₂ and N₂; time-scales for mixed-layer gas exchange with the atmosphere from wind-driven turbulence and bubbles are typically on the order of months. The oceanographic community has developed special equilibrators, with seawater showers mixing with air to measure surface-ocean CO₂ levels; these equilibrators have e-folding time-scales of roughly 30 min (e-folding, often used as the timescale characterizing a process evolving toward equilibrium, refers to the time interval in which an exponentially growing quantity increases by a factor of e). A number of engineering techniques could further reduce the CO₂/atmosphere exchange during the few minutes that water resides in the ship's hold, including: (1) limiting the ratio of air–water surface area to seawater volume, (2) limiting formation of bubbles that enhance gas exchange, and (3) limiting the turbulence on the water side (CO₂ air–water exchange is limited by water-side turbulence because the solubility of CO₂ in water is low). Notably, if the seawater's time in the ship's hold extends significantly beyond 5 min, it would become necessary to consider chemical equilibration timescales of the hydrolysis reaction between aqueous CO₂ and the larger inorganic CO₂ pool.

After nodule separation, seawater is pumped out of the collection ship's hold and injected back into the ocean in mid-water, at a depth below the euphotic zone and below the oxygen minimum layer. Any excess CO₂ contained in this returned seawater would later be released into the atmosphere at the ocean ventilation rate. The lack of any chlorofluorocarbons in water below 1000 m as well

as radiocarbon $\Delta^{14}\text{C}$ values below -180 indicate that the water is quite old; ventilation rates are over 100 years. Any CO_2 release would therefore presumably occur well after substantial reductions in anthropogenic emissions had been accomplished.

Having considered all of the above dynamics, the calculations indicate that CO_2 release from riser water does not present a serious climate change impact risk for nodule collection.

3.2.2.1.3. Mechanism 3: Land disruption. Using the nodules LCA model and SimaPro, 9800 km^2 are computed for the land competition indicator. Applying the same average carbon content yields 0.16 metric Gt of stored carbon at risk, or a maximal risk of 0.58 metric Gt of CO_2 released. Of this amount, note that 0.54 metric Gt are attributable to onshore processing, while only 0.04 metric Gt are attributable to indirect material and energy contributions for offshore collection and nodules transport to shore.

3.2.2.2. Disruption of future carbon-sequestration services. Possible harm to future sequestration of carbon could result from nodule collection if sediment disturbance compromises the rate at which abyssobenthic bacteria assimilate dissolved inorganic carbon. Research by Sweetman et al. (2018) suggests that, contrary to earlier understanding, abyssobenthic bacteria, rather than macrofauna, could be principally responsible for most carbon cycling on the CCZ abyssal seafloor. The two carbon-cycling processes performed by abyssobenthic bacteria—consuming and metabolizing phytodetritus and directly converting dissolved inorganic carbon (CO_2) into biomass by a still-unknown chemosynthetic method—had statistically indistinguishable rates.

The impact of nodule collection on the carbon-cycling functions performed by benthic bacteria is yet unclear. Bacteria living in the sediment will likely survive nodule collection and dispersal of sediment plumes, but bacteria transported to the surface in riser water will likely die as a result of lysis caused by changes in pressure and temperature (Hall et al., 2007). Additionally, if abyssobenthic bacteria require a particular spatial or structural organization to carry out their carbon-cycling functions—for example, if they need to be in an assembled layer or in contact with other organisms in some mutualistic ways—then nodule collection could disrupt their function. The mechanics, scale, and duration of these potential impacts are still unclear. Initial plowing in 1989 at the disturbance and recolonization experiment in the Peru Basin nodule field probably reduced microbial cell numbers by 50%. Twenty-six years later, the biodiversity of the microbial community was unaffected, but cell numbers were still 30% lower than pre-disturbance, leading (Vonnahme et al., 2020) to suggest that more than 50 years would be needed before biogeochemical functions returned, and that recovery could take longer in other areas with lower primary productivity, such as the CCZ.

As part of environmental-impact assessment studies required by the ISA prior to any applications for commercial exploitation of nodules, Sweetman and colleagues will carry out several years of in situ experiments in the CCZ, using respirometers and ^{13}C -labeled algae and CO_2 to quantify the amount of phytodetritus and CO_2 fixed by bacteria and archaea, the amount of bacteria grazed by fauna, and the role of bacteria as a food source for grazing or deposit feeding meiofauna, macrofauna, and megafauna. Experiments will also explore how quickly bacterial functions may recover after disturbance caused by nodule collection. If these studies confirm Sweetman et al.'s (2018) initial findings that bacteria provide approximately half of abyssobenthic carbon through chemosynthetic fixation of dissolved CO_2 , future carbon-sequestration services in the disturbed area may be substantially reduced during the time needed for recovery of full bacterial function.

To understand what could be at stake, and with Vonnahme et al.'s (2020) results in mind, assume that all abyssobenthic

bacteria living on the 508,000 km^2 area cease performing their two carbon-cycling functions for 100 years. The flux of phytodetrital particulate organic matter (POM) continues falling to the CCZ bottom at the current rate (1 g of carbon/ m^2 per year) but is not metabolized by bacteria. This carbon would remain in situ, with no method of reaching the atmosphere other than through a timescale of hundreds of millions of years of crustal-plate subduction, hence having a negligible effect on carbon sequestration. Additionally, in this scenario bacteria are no longer removing dissolved inorganic carbon from seawater. Sweetman et al. (2018) hypothesize that abyssobenthic bacteria assimilate inorganic carbon (e.g., CO_2) at a rate equivalent to about 50% (range 31–57%) of the incoming POM. Those bacteria would normally sequester ~ 0.5 g of carbon/ m^2 from seawater annually, or 0.025 metric Gt over 100 years. Without their function, this carbon would remain in the water column, creating a slightly “carbon-enriched” deep seawater. However, slightly carbon-enriched deep seawater would not slow oceanic absorption of atmospheric CO_2 for long, since CO_2 is only absorbed from the atmosphere at the ocean surface, or 4–6 km above the CCZ seafloor. It would take centuries or millennia for the slightly carbon-enriched deep water to reach the surface via thermohaline circulation. The resulting retardation in the rate of oceanic absorption of CO_2 would be relatively miniscule. Still, under this extreme scenario of obliterated carbon-sequestration function for 100 years in all seabed areas impacted by nodule collection, 0.025 metric Gt of carbon, equivalent to 0.09 metric Gt of CO_2 , would not be sequestered.

In the face of uncertainty around abyssobenthic carbon cycling, it is important to understand the global significance of this potential disruption of future carbon-sequestration services. The area of the CCZ currently under exploration contracts is 1.2 million km^2 , with another 1.44 million km^2 set aside by the ISA into areas under environmental protection (ISA, 2019). The total area being explored for polymetallic nodules in the CCZ represents 0.4% of the overall area of oceanic abyssal sediments of 270 million km^2 . The allocated seabed area needed to supply the base metals for producing 1 billion EV batteries is 0.5 million km^2 or 0.2% of global abyssal sediments. If nodule collection severely disrupted the carbon-cycling services provided by abyssobenthic bacteria, it would likely impact 0.2% of the global service capacity.

Finally, the same land procedure is applied to nodules' 9800 km^2 LCIA land footprint. This area includes indirect contributions from offshore material production, but the overwhelming contribution comes from onshore processing. This land area results in an additional 0.04 metric Gt of carbon (0.15 metric Gt of CO_2), for a total of 0.065 metric Gt of carbon (0.24 metric Gt of CO_2) not sequestered over a 100-year period due to nodule collection and processing. Notably, the sequestration disruption attributable to nodules' relatively small land footprint—which is primarily from onshore processing—appears greater than the total disruption in the sea: over 60% of the total 0.065 metric Gt of disrupted carbon is attributable to the 9800 km^2 LCIA land area.

3.2.3. Uncertainties in carbon-sequestration impact estimates

For land ores, uncertainty in the carbon-sequestration analysis primarily arises from the use of globally averaged data. Without a granular database documenting localized data associated with mining projects—such as soil and vegetation carbon content, razed forests, and as-implemented impact-mitigation strategies—attaining a precise answer is challenging, and high-level estimation methodologies need to be used. The carbon released could somewhat lessen if there is widespread adoption of soil-burial practices, in which topsoil is carefully excavated and stored to reduce carbon loss and preserve microflora, soil invertebrates, and soil health for later use in site reclamation (Brown et al., 2008),

or if dead wood or fresh vegetation cut during land clearing can be buried in trenches or stored long term, such that decomposition and carbon loss is substantially reduced for very long periods (Zeng, 2008). Brown et al.'s (2008) study taken with Trumper et al. (2009) suggests soil could otherwise take 700 years to fully regain its original carbon content. The time frame for restoration of affected services if left unremediated is also a topic for further study; the 100-year scenario was based on an assumption of active and full restoration of sites, but execution is known to be inconsistent across the industry.

For nodules' riser-water impact, some uncertainty exists about temperature gradients during the water's journey, exposure time, and exposure volumes. Design impacts may vary by final specifications of the collector vehicles, riser pipe, and off-loading processes. If water's exposure to air varies from assumptions by a significant amount, e.g., an order of magnitude, then additional dynamics might come into play. To test the sensitivity to riser-water temperature increases, the United States Geological Survey's CO2calc program (Robbins et al., 2010) was used with the same seawater chemistry and operational-system parameters but varying the temperature differentials from 6 °C to 12 °C. The annual CO2 flux increased by up to 38% under the extreme case. Such variations in riser-water-driven impact are still dwarfed by seafloor disruption and the land-footprint contribution. For nodules' seafloor-disruption impact, uncertainty arises primarily in understanding abyssobenthic bacterial regrowth dynamics, particularly the timelines and asymptotic restoration properties. Ongoing environmental-impact assessment studies will provide more data on this question.

3.2.4. Carbon-sequestration impact summary

The GWP impact differences we saw earlier, however significant, are dwarfed by the much larger potential impact differences on carbon-sequestration cycles, driven primarily by land transformation. The findings suggest that nodule collection and processing operations are unlikely to release substantial amounts of already-sequestered carbon into the atmosphere. Amounts at risk of release are an order of magnitude lower compared to land-ore mining methods and are almost entirely attributable to the land footprint of processing nodules onshore (Table 6). Assuming no recovery of vegetation on mined land and no recovery of chemosynthetic bacterial flora on the CCZ seafloor for 100 years, the amount of carbon-sequestration service sacrificed to make metals for 1 billion EVs would be eight times higher using land mining compared to nodules (Table 7). Impacts would be equivalent if all chemosynthetic bacterial flora on the CCZ seafloor did not recover for 2000 years, which is highly unlikely given the abundance of abyssobenthic bacteria in deep-sea sediments, pore water, and left-behind nodule cover, as well as suspended in water.

4. Conclusion and future prospects

Avoiding catastrophic effects of climate change requires the

Table 6
Estimated sequestered carbon potentially at risk of release when producing metals for 1 billion EVs.

Mechanism for releasing sequestered carbon	Carbon at risk (metric Mt CO ₂)	
	Land ores	Nodules
Mechanism 1: Seabed disruption	0	2.8
Mechanism 2: Riser water	0	0.15
Mechanism 3: Land disruption	9300	580
Total	9300	583

Table 7
Carbon-sequestration services performed over 100 years by land and seabed footprints that would be disrupted by metal production for 1 billion EVs.

Footprint type	Carbon sequestered over 100 years (metric Mt CO ₂)	
	Land ores	Nodules
Land	2060	151
Seabed	0	93
Total	2060	244

planet to transition to a renewable-energy infrastructure. Constructing that infrastructure requires a substantial increase in metal supplies, prompting a new wave of exploration worldwide. Recycling and circular-economy approaches should be pursued aggressively, but it is infeasible to fully rely on them in the short term, as they are unlikely to meet the full demand prospects of green-technology upscaling needed to meet the Paris Agreement's emissions-reduction targets (Ali et al., 2017). As an alternative to expanding the supply of ores from traditional mines on land to meet this demand, seabed mineral resources deserve attention, particularly given the upcoming development of regulations by the ISA under the UNCLOS (Sovacool et al., 2020). Consonant with global goals for sustainability (UN, 2015), in determining the choice of mineral supply, all stakeholders, including manufacturers, consumers, and governments, should consider the environmental and social consequences of extraction, in tandem with economic considerations.

Here, a comprehensive comparative analysis of climate change impacts showed a substantially lower footprint when using nodules. Conscious of the numerous uncertainties in key technologies being developed for carbon mitigation in mineral production, an aggressive, global-grid decarbonization scenario was built into the analysis. Even in that possible future, this study's results imply that deep-sea polymetallic nodules, if properly managed with appropriate governance safeguards, have the potential for delivering a much cleaner source of key technology metals than land ores.

The next step is to consider sustainability impacts more broadly, such as waste, impacts on water sources, and social impacts. The use of polymetallic nodules in fact could reduce the production of wastes, tailings, dusts, and associated pollution of land, water, and air; substantially reduce freshwater use; substantially reduce human fatalities, injuries, and health effects associated with traditional open-pit and underground mining as well as tailings-dam collapses; avoid harming indigenous cultures; and avoid child labor (Paulikas et al., 2020). A separate question is whether a new supply of nodule-derived metals could indirectly impact aggregate metal consumption, nudge investments in recycling technology and infrastructure, or have policy externalities. Such determinations should be weighed in tandem with the social and environmental benefits of using nodules. Sourcing battery metals from oceanic nodules would not likely replace all terrestrial mining for nickel, cobalt, manganese, and copper, but it could retard the spread of mining into virgin areas and depress production of the lowest-grade ores, which typically have the highest social and environmental impacts.

Future studies may expand upon these results by modeling additional representative metallurgical pathways for nodule processing since it is the dominant GWP-contributing phase, and adding data refinements once nodule-processing designs are finalized and operational data become available. The land-ore baseline should also be updated as new studies of relevant pathways become available. Any future analyses may be aided significantly if the land-ore mining industry assembled databases for a

representative sample of mines, from various climate and ecological regions, detailing estimates of the amount of land cleared, carbon contents of cleared soil and vegetation, strategies employed (if any) to reduce loss of sequestered carbon, and results over time of the implemented strategies. Such data would help future researchers reduce reliance on coarse data and assumptions, enabling computation of increasingly accurate estimates of the climate effects of mining. Such databases detailing strategies and results of emissions-reduction efforts would be important demonstrations of industrial progress toward global agreements on climate mitigation. Similarly, DSM companies should be charged with providing data on the climate effects of their activities if commercial exploitation occurs. Operators are encouraged to baseline their own impacts, and to make environmentally conscious choices that drive down impact; they should also consider imposing renewable-electricity access as a chief plant-site selection criterion. Industrial purchasers of battery metals should consider the land-ores versus nodule results, as well as review individual contractors' impact baselines, when setting their supply-chain strategies. By following a rigorous life cycle analysis approach, better-informed decisions about cleaner production methods can be achieved.

CRedit authorship contribution statement

Daina Paulikas: Conceptualization, Data curation, Methodology, Investigation, Software, Visualization, Validation, Writing - original draft. **Steven Katona:** Conceptualization, Data curation, Methodology, Investigation, Writing - original draft. **Erika Ilves:** Conceptualization, Methodology, Validation, Writing - review & editing, Funding acquisition, Resources, Project administration, Supervision. **Saleem H. Ali:** Writing - review & editing, Supervision.

Declaration of competing interest

The authors declare the following financial interests/personal relationships which may be considered as potential competing interests: This research is a product of independent inquiry that was funded by DeepGreen Metals Inc., Vancouver, Canada, which is planning to embark on mining of deep-sea polymetallic nodules in the CCZ. Erika Ilves is also Head of Strategy for DeepGreen Metals. In addition to funding, DeepGreen Metals provided access to data and expertise in terrestrial mining processes and deep-sea mining techniques.

Acknowledgements

We gratefully acknowledge the helpful inputs and reviews from many who contributed to this project, including academic reviews and guidance from Dr. Todd Cort, Dr. Scott Doney, Dr. Matthew Eckelman, Cary Krosinsky, Dr. Susan Letcher, Arvydas Paulikas, Dr. Lisa Robbins, and Dr. Laurant van Oers, and DeepGreen support and expertise from Dr. Jeffrey Donald, Anthony O'Sullivan, Dan Porras, and Dr. Greg Stone.

Appendix A. Supplementary data

Supplementary data to this article can be found online at <https://doi.org/10.1016/j.jclepro.2020.123822>.

Abbreviations/nomenclature

ANL	Argonne National Laboratory
CCZ	Clarion Clipperton Zone
CI	Cobalt Institute

CML	Centrum voor Milieuwetenschappen (Institute of Environmental Sciences)
Co	cobalt
CO ₂	carbon dioxide
CO ₂ e	CO ₂ equivalent
Cu	copper
DRC	Democratic Republic of the Congo
EMM	electrolytic manganese metal
EV	electric vehicle
GEO	Global Environmental Outlook
Gt	gigaton
GWP	global warming potential
IEA	International Energy Agency
IPCC	International Panel on Climate Change
ISA	International Seabed Authority
kg	kilogram
km	kilometer
LCA	life cycle assessment
LCI	life cycle inventory
LCIA	life cycle impact assessment
LCSA	life cycle sustainability assessment
Ni	nickel
Mn	manganese
Mt	megaton
NH ₄	ammonium
POM	particulate organic matter
SiMn	silicomanganese
SO ₄	sulfate
UN	United Nations
UNCLOS	United Nations Convention on the Law of the Sea
UNEP	United Nations Environment Programme
USGS	United States Geological Survey
WEO	World Energy Outlook

References

- Ali, S.H., Giurco, D., Arndt, N., Nickless, E., Brown, G., Demetriades, A., Durrheim, R., et al., 2017. Mineral supply for sustainable development requires resource governance. *Nature* 543 (7645), 367–372. <https://doi.org/10.1038/nature21359>.
- AMC Consultants, 2019a. NORI Area D Clarion Clipperton Zone Mineral Resource Estimate.
- AMC Consultants, 2019b. Preliminary Economic Assessment of the NORI Area D Project, Clarion Clipperton Zone.
- AMY, 2018. AMY Business Plan. December 14. <https://americanmanganeseinc.com/investor-info-2/amy-business-plan/>. (Accessed 3 June 2019).
- Ayres, R.U., Ayres, L.W., Rade, I., 2002. The life cycle of copper, its co-products and byproducts. *J. Ind. Ecol.* 24 <https://doi.org/10.1162/108819899569458>.
- Bloomberg New Energy Finance, 2020. Electric Vehicle Outlook 2020. Bloomberg. <https://about.bnef.com/electric-vehicle-outlook/>.
- Brown, S., Trlica, A., Teshima, M., 2008. Carbon sequestration potential on mined lands. In: Bolan, N.S., Kirkham, M.B., Ok, Y.S. (Eds.), Chap. 11 in *Spoil To Soil: Mine Site Rehabilitation And Revegetation*. CRC Press, pp. 189–201.
- Ciais, P., Sabine, C., Bala, G., Bopp, L., Brovkin, V., Canadell, J., Chhabra, A., et al., 2013. Carbon and other biogeochemical cycles. In: Stocker, T.F., Qin, D., Plattner, G.K., Tignor, M., Allen, S.K., Boschung, J., Nauels, A., Xia, Y., Bex, V., Midgley, P.M. (Eds.), *Climate Change 2013: the Physical Science Basis. Contribution of Working Group I to the Fifth Assessment Report of the IPCC*. Cambridge University Press, Cambridge, UK and NY, NY, USA. https://www.ipcc.ch/site/assets/uploads/2018/02/WG1AR5_Chapter06_FINAL.pdf.
- Classen, M., et al., 2009. Life Cycle Inventories of Metals. Dubendorf: Ecoinvent v2.1 Report No. 10.
- Cobalt Institute, 2016. Life Cycle Assessment of Cobalt. <https://www.cobaltinstitute.org/life-cycle-assessment.html>.
- Cru International, 2019. Market Overviews for DeepGreen Preliminary Economic Assessment.
- Dai, Q., Kelly, J.C., Elgowainy, A., 2018. Cobalt Life Cycle Analysis Update for the GREET Model. Systems Assessment Group. Energy Systems Division, Argonne National Laboratory.
- Ecoinvent, 2018. Ammonium Sulfate, as N {GLO} | Nickel Mine Operation, Sulfidic Ore | Cut-Off. U. Ecoinvent database version 3.0.87.0.
- Ecoinvent, 2020. Ecoinvent version 2. <https://www.ecoinvent.org/database/older-versions/ecoinvent-version-2/ecoinvent-version-2.html>. (Accessed 22 January 2020).
- EEA, 2015. Soil and Climate Change: Signals 2015. European Environment Agency.

- June 30. <https://www.eea.europa.eu/signals/signals-2015/articles/soil-and-climate-change>.
- Elias, F., Ferreira, J., Lennox, G.D., Berenguer, E., Ferreira, S., Schwartz, G., de Oliveira Melo, L., et al., 2020. Assessing the growth and climate sensitivity of secondary forests in highly deforested Amazonian landscapes. *Ecology* 101 (3), e02954. <https://doi.org/10.1002/ecy.2954>.
- Erb, K., Kastner, T., Plutzer, C., Bais, A.L.S., Carvalhais, N., Fetzel, T., Gingrich, S., et al., 2018. Unexpectedly large impact of forest management and grazing on global vegetation biomass. *Nature* 553, 73–76. <https://doi.org/10.1038/nature25138>.
- FAO, 2010. Global Forest Resources Assessment 2010 Main Report. Food and Agriculture Organization of the United Nations, Rome. <http://www.fao.org/3/a-i1757e.pdf>.
- Farjana, S.H., Huda, N., Mahmud, M.A.P., 2019. Life cycle assessment of cobalt extraction process. *J. Sustain. Min.* <https://doi.org/10.1016/j.jsm.2019.03.002>.
- Girotra, P., Sing, S.K., Nagpal, K., 2012. Supercritical fluid technology: a promising approach in pharmaceutical research. *Pharmaceut. Dev. Technol.* 18 (1) <https://doi.org/10.3109/10837450.2012.726998>.
- Greenpeace, 2019. In Deep Water: the Emerging Threat of Deep Sea Mining. Greenpeace International. <https://www.greenpeace.org/international/publication/22578/deep-sea-mining-in-deep-water/>.
- Guinee, J., 2016. Life cycle sustainability assessment: what is it and what are its challenges? In: Clift, R., Druckman, A. (Eds.), *Taking Stock of Industrial Ecology*. Springer International, Cham, Switzerland.
- Guinee, J., Gorree, M., Heijungs, R., 2002. Handbook on Life Cycle Assessment. Kluwer Academic Publishers. <http://www.lavoisier.fr/livre/notice.asp?id=PKOW30AO33SOWT>.
- Hall, P.O.J., Brunnegard, J., Hulthe, G., Martin, W.R., Stahl, H., Tengberg, A., 2007. Dissolved organic matter in abyssal sediments: core recovery artifacts. *Limnol. Oceanogr.* 52 (1), 19–31. <https://aslopubs.onlinelibrary.wiley.com/doi/epdf/10.4319/lo.2007.52.1.0019>.
- Hatch, 2014. Lifecycle Assessment of Global Manganese Alloy Production. International Manganese Institute, Paris. <http://www.manganese.org>.
- Hausfather, Z., 2019. Factcheck: how electric vehicles help tackle climate change. Carbon Brief. May 13. <https://www.carbonbrief.org/factcheck-how-electric-vehicles-help-to-tackle-climate-change>.
- Haynes, B.W., Law, S.L., Barron, D.C., Kramer, G.W., Maeda, R., Magyar, M.J., 1985. Pacific Manganese Nodules: Characterization and Processing. United States Department of the Interior Bureau of Mines, Bulletin, Washington, D. C.
- Heil, A., 2018. Ammonium Sulfate, as N [RER] Ammonium Sulfate Production | Cut-Off, U. Ecoinvent database version 3.0.89.1.
- Hein, J.R., Koschinsky, A., Kuhn, T., 2020. Deep-ocean polymetallic nodules as a resource for critical materials. *Nature Rev. Earth & Environ.* <https://doi.org/10.1038/s43017-020-0027-0>.
- Heinrich, L., Koschinsky, A., Markus, T., Singh, P., 2020. Quantifying the fuel consumption, greenhouse gas emissions and air pollution of a potential commercial manganese nodule mining operation, 114, 103678. <https://doi.org/10.1016/j.marpol.2019.103678>, 2020.
- Hester, K.C., Brewer, P.G., 2009. Clathrate hydrates in nature. *Ann. Rev. Marine Sci.* 1, 303–327. <https://doi.org/10.1146/annurev.marine.010908.163824>.
- Howard, P., Parker, G., Jenner, N., Holland, T., 2020. An Assessment of the Risks and Impacts of Seabed Mining on Marine Ecosystems. Fauna & Flora International, London. https://cms.fauna-flora.org/wp-content/uploads/2020/03/FFI_2020_The-risks-impacts-deep-seabed-mining_Report.pdf.
- Hund, K., La Porta, D., Fabregas, T.P., Drexhage, J., 2020. Minerals for Climate Action: the Mineral Intensity of the Clean Energy Transition. World Bank Group, Washington, D. C. <http://pubdocs.worldbank.org/en/961711588875536384/Minerals-for-Climates-Action-The-Mineral-Intensity-of-the-Clean-Energy-Transition.pdf>.
- ICSG, 2015. International Copper Study Group 2015 Statistical Yearbook. Lisbon.
- IEA, 2012. World Energy Outlook. OECD International Energy Agency. <http://worldenergyoutlook.org/publications/weo-2012/>.
- IPCC, 2018. Summary for Policymakers of IPCC Special Report on Global Warming of 1.5C Approved by Governments. <https://www.ipcc.ch/2018/10/08/summary-for-policymakers-of-ipcc-special-report-on-global-warming-of-1-5c-approved-by-governments/>.
- ISA, 2019. Deep Seabed Minerals Contractors. International Seabed Authority. <https://www.isa.org/jm/deep-seabed-minerals-contractors/overview>.
- Jones, D.O.B., Kaiser, S., Sweetman, A.K., 2017. Biological responses to disturbance from simulated deep-sea polymetallic nodule mining. *PLoS ONE*. <https://doi.org/10.1371/journal.pone.0171750>.
- Keenan, T.F., Williams, C.A., 2018. The terrestrial carbon sink. *Annu. Rev. Environ. Resour.* 43, 219–243. <https://doi.org/10.1146/annurev-environ-102017-030204>.
- Krauss, U., Wagner, H., Atmaca, T., Neumann, W., Al, E., 1999. Stoffmengenflüsse und Energiebedarf bei der Gewinnung ausgewählter mineralischer Rohstoffe: Teilstudie Kupfer. Hannover.
- Kuipers, K.J.J., van Oers, L.F.C.M., Verboon, M., van der Voet, E., 2018. Assessing environmental implications associated with global copper demand and supply scenarios from 2010 to 2050. *Global Environ. Change* 49, 106–115.
- Lal, R., 2004. Soil carbon sequestration impacts on global climate change and food security. *Science* 304 (5677), 1623–1627. <https://doi.org/10.1126/science.1097396>.
- Levin, L.A., Baco, A.R., Bowen, D.A., Colaco, A., Cordes, E.E., Cunha, M.R., Demopoulos, A.W.J., et al., 2016. Hydrothermal vents and methane seeps: rethinking the sphere of influence. *Front. Marine Sci.* <https://doi.org/10.3389/fmars.2016.00072>.
- Levova, T., 2016a. Manganese Dioxide [GLO] | Production | Cut-Off, U. Ecoinvent Database Version 3.0.1.0.
- Levova, T., 2016b. Manganese Sulfate [GLO] | Production | Cut-Off, U. Ecoinvent Database Version 3.0.1.0.
- Liu, S., Wei, Y., Post, W.M., Cook, R.B., Schaefer, K., Thornton, M.M., 2013. The Unified North American Soil Map and its implication on the soil organic carbon stock in North America. *Biogeosciences* 10, 2915–2930. <https://www.biogeosciences.net/10/2915/2013/bg-10-2915-2013.html>.
- Lu, X., Kicklighter, D.W., Melillo, J.M., Reilly, J.M., Xu, L., 2015. Land carbon sequestration within the conterminous United States: regional- and state-level analyses. *J. Geophys. Res.: Biogeosciences* 120 (2), 379–398. <https://doi.org/10.1002/2014JG002818>.
- Morgan, C.L., 2000. Resource estimates of the Clarion Clipperton manganese nodule deposits. In: *Handbook of Marine Mineral Deposits*, pp. 145–170.
- Morgan Stanley, 2017. Race for battery-electric vehicle sales: global passenger car fleet. <http://res.cloudinary.com/yumyoshojin/image/upload/v1/pdf/future-transport-2018.pdf>.
- National Snow and Ice Data Center, 2020. Facts about glaciers. <https://nsidc.org/cryosphere/glaciers/quickfacts.html>. (Accessed 22 January 2020).
- Nauels, A., Rosen, D., Mauritsen, T., Maycock, A., McKenna, C., Rogelj, J., Schleussner, C.-F., Smith, E., Smith, C., Forster, P., 2019. Zero IN on the Remaining Carbon Budget and Decadal Warming Rates. EU CONSTRAIN 2019 Project. <https://climateanalytics.org/publications/2019/zero-in-on-the-remaining-carbon-budget-and-decadal-warming-rates/>.
- Norgate, T.E., 2001. A Comparative Life Cycle Assessment of Copper Production Processes. CSIRO Minerals.
- Norgate, T.E., Haque, N., 2010. Energy and greenhouse gas impacts of mining and material processing operations. *J. Clean. Prod.* 18 (3), 266–274.
- Norgate, T.E., Jahanshahi, S., Rankin, W.J., 2007. Assessing the environmental impact of metal production processes. *J. Clean. Prod.* 15 (8–9), 838–848. <http://linkinghub.elsevier.com/retrieve/pii/S0959652606002320>.
- Norgate, T.E., Lovel, R.R., 2006. Sustainable water use in minerals and metal production. In: *Green Processing Conference*. Newcastle, pp. 133–141.
- Norgate, T.E., Rankin, W.J., 2000. Life cycle assessment of copper and nickel production. In: *International Conference on Minerals Processing and Extractive Metallurgy (MINPREX)*. Melbourne, pp. 133–138. http://www.minerals.csiro.au/sd/CSIRO_Paper_LCA_CuNi.htm.
- Nuss, P., Eckelman, M.J., 2014. Life cycle assessment of metals: a scientific synthesis. *PLoS ONE* 9 (7).
- Paulikas, D., Katona, S., Ilves, E., Stone, G., O'Sullivan, G., 2020. Where should metals for the green transition come from? <https://deep.green/white-paper/>.
- Peng, X., Yu, H., Wang, P., Liu, Y., Yang, L., Dong, H., Ren, Y., Wang, H., 2012. Production assessment in the electrolytic manganese metal industry in China. *Rev. Metall.* 108, 437–442. <https://doi.org/10.1051/metal/2011073>.
- Pre Consultants, 2020. SimaPro: LCA software for fact-based sustainability. <https://simapro.com/>. (Accessed 22 January 2020).
- Rainforest Action Network, 2020. Indonesia's rainforests: biodiversity and endangered species. https://www.ran.org/indonesia_s_rainforests_biodiversity_and_endangered_species/. (Accessed 20 January 2020).
- Robbins, L.L., Hansen, M.E., Kleypas, J.A., Meylan, S.C., 2010. CO2calc: A User-Friendly Seawater Carbon Calculator for Windows, Mac OS X, and iOS (iPhone). Version 4.0.9, U.S. Geological Survey Open-File Report 2010–1280, p. 17. <https://pubs.usgs.gov/of/2010/1280/>.
- Romboll IMS HWWV, 2016. Analyse des volkswirtschaftlichen Nutzens der Entwicklung eines kommerziellen Tiefseebergbaus in den Gebieten, denen Deutschland Explorationslizenzen der Internationalen Meeresbodenbehörde besitzt burg. Bundesministeriums für Wirtschaft und Energie, Hamburg, Germany.
- Secretariat of the Pacific Community, 2013. Deep Sea Minerals: manganese Nodules, a physical, biological, environmental, and technical review. In: Baker, E., Beaudoin, Y. (Eds.), Secretariat of the Pacific Community, 1B. http://dsm.gsd.spc.int/public/files/meetings/TrainingWorkshop4/UNEP_vol1B.pdf.
- Sovacool, B.K., Ali, S.H., Bazilian, M., Radley, B., Nemery, B., Okatz, J., Mulvaney, D., 2020. Sustainable minerals and metals for a low-carbon future. *Science* 367 (6473), 30–33. <https://doi.org/10.1126/science.aaz6003>.
- Sweetman, A.K., Smith, C.R., Shulse, C.N., Maillot, B., Lindh, M., Church, M.J., Meyer, K.S., van Oevelen, D., Stratmann, T., Gooday, A.J., 2018. Key role of bacteria in the short-term cycling of carbon at the abyssal seafloor in a low particulate organic carbon flux region of the eastern Pacific Ocean. *Limnol. Oceanogr.* 64, 694–713. <https://doi.org/10.1002/lno.11069>.
- Tardy, Y., 1997. Translated by. In: Sarma, V.A.K. (Ed.), *Petrology of Laterites and Tropical Soils*. A.A. Balkema, Rotterdam.
- Trumper, K., Bertzy, M., Dickson, B., van der Heijden, G., Jenkins, M., Manning, P., 2009. The Natural Fix? the Role of Ecosystems in Climate Mitigation. A UNEP Rapid Response Assessment. United Nations Environment Programme, Cambridge, UK. https://gridarendal-website-live.s3.amazonaws.com/production/documents/s_document/226/original/BioseqRRA_scr.pdf?1486734377.
- UN, 2015. Transforming Our World: the 2030 Agenda for Sustainable Development. A/RES/70/1. Resolution adopted by the UN General Assembly 25 September 2015. <https://sustainabledevelopment.un.org/content/documents/21252030%20Agenda%20for%20Sustainable%20Development%20web.pdf>.
- UNEP, 2007. Global Environment Outlook (GEO-4): environment for development. <http://www.resourcepanel.org/reports>. (Accessed 28 November 2017).
- USGS, n.d. "Where Are Hydrates Found." US Geological Service. Accessed February 20, 2020. https://www.usgs.gov/faqs/where-are-gas-hydrates-found?qt-news_

- science_products=0#qt-news_science_product.
- van der Voet, E., van Oers, L., Verboon, M., Kuipers, K., 2018. Environmental implications of future demand scenarios for metals. *J. Ind. Ecol.* <https://doi.org/10.1111/jiec.12722>.
- Verboon, M., 2016. *Environmental Impacts of Nickel Production, 2010 - 2050: An Assessment of the Environmental Impacts of Metal Demand and Supply Scenarios Using Life Cycle Assessment*. MSc Industrial Ecology Thesis. Leiden University & Delft University of Technology, Den Haag, Netherlands.
- Volz, J.B., Mogollón, J.M., Geiberta, W., Martinez Arbizue, P., Koschinsky, A., Kastenag, S., 2018. Natural spatial variability of depositional conditions, biogeochemical processes and element fluxes in sediments of the eastern Clarion-Clipperton Zone, Pacific Ocean. *Deep Sea Res. Oceanogr. Res. Pap.* 140, 159–172. <https://doi.org/10.1016/j.dsr.2018.08.006>.
- Vonnahme, T.R., Molari, M., Janssen, F., Wenzhofer, F., Haeckel, M., Titschack, J., Boetius, A., 2020. Effects of a deep-sea mining experiment on seafloor microbial communities and functions after 26 years. *Sci. Adv.* <https://doi.org/10.1126/sciadv.aaz5922>.
- Westfall, L.A., Davourie, J., Ali, Mohammed, McGough, D., 2016. Cradle-to-gate life cycle assessment of global manganese alloy production. *Int. J. Life Cycle Assess.* (21), 1573–1579. <https://doi.org/10.1007/s11367-015-0995-3>.
- Wikipedia, 2019. Earth. <https://en.wikipedia.org/wiki/Earth>. (Accessed August 2019).
- World Ocean Review, 2010. The oceans – the largest CO₂-reservoir. Living with the oceans. A report on the state of the world's oceans. *World Ocean Rev.* <https://worldoceanreview.com/en/wor-1/ocean-chemistry/co2-reservoir/>.
- Yang, Y., 2017. Beyond the conventional "life cycle" assessment. *Biofuel Res. J.* 15, 637. <https://doi.org/10.18331/BRJ2017.4.3.2>, 2017.
- You, K., Flemings, P.B., Malinverno, A., Collett, T.S., Darnell, K., 2019. Mechanisms of methane hydrate formation in geological systems. *Rev. Geophys.* 57, 1146–1196. <https://doi.org/10.1029/2018RG000638>.
- Zeng, N., 2008. Carbon sequestration via wood burial. *Carbon Bal. Manag.* 3 (1) <https://doi.org/10.1186/1750-0680-3-1>.
- Zhang, R., Ma, X., Shen, X., Zhai, Y., Zhang, T., Ji, C., Hong, J., 2020. Life cycle assessment of electrolytic manganese metal production. *J. Clean. Prod.* 253 <https://doi.org/10.1016/j.jclepro.2019.119951>.
- Zomer, R.J., Bossio, D.A., Sommer, R., Verchot, L.V., 2017. Global sequestration potential of organic carbon in cropland soils. *Sci. Rep.* 7, 15554. <https://doi.org/10.1038/s41598-017-157494-8>.